https://doi.org/10.5194/egusphere-2024-626
Preprint. Discussion started: 5 March 2024

Temperature effect on seawater fCO_2 revisited: theoretical basis, uncertainty analysis, and implications for parameterising carbonic acid equilibrium constants

Matthew P. Humphreys

Department of Ocean Sciences, NIOZ Royal Netherlands Institute for Sea Research, PO Box 59, 1790 AB Den Burg (Texel), the Netherlands

Correspondence to: Matthew P. Humphreys (matthew.humphreys@nioz.nl)

Abstract. The sensitivity of the fugacity of carbon dioxide in seawater (fCO_2) to temperature (denoted υ, reported in % °C^{-1}) is critical for the accurate fCO_2 measurements needed to build global carbon budgets and for understanding the drivers of air-sea CO_2 flux variability across the global ocean. Yet understanding and computing this property have until now been restricted to either using purely empirical functions fitted to experimental data or determining it as an emergent property of a fully resolved marine carbonate system, and these two approaches are not consistent with each other. The lack of a theoretical basis and an uncertainty estimate for υ has hindered resolving this discrepancy. Here, we develop a new approach to calculating the temperature sensitivity of fCO_2 based on the equations governing the marine carbonate system and the van 't Hoff equation. This shows that $\ln(fCO_2)$ should be proportional to $1/t_K$ (where t_K is temperature in K) to first order, rather than to temperature as has previously been assumed. Our new approach is consistent with experimental data, although more measurements are needed to confirm this, particularly at temperatures above 25 °C. It is consistent with field data, performing better than any other approach for adjusting fCO_2 data by up to 10 °C. It is also consistent with calculations from a fully resolved marine carbonate system, which we have incorporated into the PyCO2SYS software. The uncertainty in υ arising from only measurement uncertainty in the scarce experimental data with which υ has been directly measured is on the order of 0.04% °C^{-1}, which corresponds to a 0.04% uncertainty in fCO_2 adjusted by +1 °C. However, spatiotemporal variability in υ is several times greater than this, so the true uncertainty due to the temperature adjustment in fCO_2 adjusted by +1 °C using the most widely used constant υ value is around 0.24%. This can be reduced to around 0.06% by using the new approach proposed here, and this could be further reduced with more measurements. The spatiotemporal variability in υ arises from the equilibrium constants for CO_2 solubility and carbonic acid dissociation (K_1^* and K_2^*) and its magnitude varies significantly depending on which parameterisation is used for K_1^* and K_2^*. Seawater fCO_2 can be measured accurately enough that additional experiments should be able to detect spatiotemporal variability in υ and distinguish between the different parameterisations for K_1^* and K_2^*. Because the most widely used constant υ was coincidentally measured from seawater with roughly global average υ, our results are unlikely to significantly affect global air-sea CO_2 flux budgets, but may have more important implications for regional budgets and studies that adjust by larger temperature differences.

https://doi.org/10.5194/egusphere-2024-626
Preprint. Discussion started: 5 March 2024

1 Introduction

The surface ocean continuously exchanges carbon dioxide (CO_2) with the atmosphere. The net direction of exchange varies through space and time, with some ocean areas acting as CO_2 sources and others as sinks (Takahashi et al., 2009). Whether an area acts as a CO_2 source or sink depends on the difference between the fugacity of CO_2 (fCO_2) in the sea and in the air (denoted $\Delta fCO_2 = fCO_2(sea) - fCO_2(air)$), with net CO_2 transfer from high to low fCO_2. The fugacity of CO_2 is similar to its partial pressure (pCO_2) but with a small correction for the non-ideal behaviour of CO_2 in air; fCO_2 is typically about 99.7% of pCO_2. The gas exchange rate is modulated by a set of processes that are commonly parameterised as a function of wind speed (Wanninkhof, 2014). Most of the surface ocean is either a CO_2 source or sink, rather than being in equilibrium with the atmosphere, because many of the processes that modify seawater fCO_2 (e.g., seasonal cycles of temperature and primary productivity) operate on faster timescales than air-sea CO_2 equilibration, which takes from months to a year for the surface mixed layer (Jones et al., 2014).

On top of the natural background variability, the global ocean is a net CO_2 sink due to rising atmospheric fCO_2. About a quarter of the anthropogenic CO_2 emitted each year, some 2.8 ± 0.4 Gt-C in 2022, is taken up by the ocean, mitigating the greenhouse effect of CO_2 on Earth's climate (Friedlingstein et al., 2023). Together, uptake of CO_2 and warming drive changes in the marine carbonate system, altering biologically important variables like seawater pH and the saturation states with respect to carbonate minerals (Humphreys, 2017). Quantifying marine CO_2 uptake requires highly accurate fCO_2 measurements: it is driven by a global mean ΔfCO_2 of less than 10 µatm, which is around 2% of mean fCO_2. Consequently, small systematic biases in seawater fCO_2 propagate into large errors in ΔfCO_2 and thus the total ocean CO_2 sink. The required measurement accuracy has been quantified by the Global Ocean Acidification Observing Network (GOA-ON), who suggested a minimum accuracy of 0.5% for "climate quality" seawater fCO_2 measurements that can be used to detect decadal trends or 2.5% for "weather quality" fCO_2 data for investigating changes of greater magnitude, such as seasonal cycles (Newton et al., 2015).

The observational constraint on marine CO_2 uptake is based on measurements of surface ocean fCO_2 from ships, compiled into data products such as the Surface Ocean CO_2 Atlas (SOCAT; Bakker et al., 2016). Surface seawater is pumped through to a measuring device and the raw measurements are passed through a series of processing steps to obtain seawater fCO_2. One important processing step is the temperature adjustment. While it is being pumped from the surface ocean to the measuring device, seawater may warm up or cool down. As fCO_2 is highly sensitive to temperature (Weiss, 1974), each measurement must be adjusted back to its in situ temperature in order to obtain environmentally relevant values of fCO_2 (Pierrot et al., 2009; Pfeil et al., 2013; Goddijn-Murphy et al., 2015). For the data in SOCAT, a maximum change in temperature (Δt) of 1 °C between intake and measurement is permitted (although in practice, adjustments are usually around 0.2-0.3 °C; Wanninkhof et al., 2022), in order to minimise uncertainty in fCO_2 due to the temperature adjustment, but adjustments with greater Δt are often used in other applications. For example, several studies have normalised seawater fCO_2 observations to a constant temperature in order to investigate the non-thermal (i.e., chemical) drivers of fCO_2 change on various timescales

https://doi.org/10.5194/egusphere-2024-626
Preprint. Discussion started: 5 March 2024

(e.g., Takahashi et al., 2002, 2003, 2006; Feely et al., 2006). Others have computed the temperature sensitivity in order to isolate the thermal component of observed fCO_2 change and unravel the drivers of fCO_2 variability (e.g., Metzl et al., 2010). Data from SOCAT have been adjusted from the intake temperature, typically measured a few metres below the sea surface, to the temperature directly at the sea surface in order to assess how the "cool skin" effect affects computed air-sea CO_2 fluxes (e.g., Watson et al., 2020; Dong et al., 2022). Finally, climatological fCO_2 datasets have been adjusted to match different sea surface temperature fields for specific analyses (e.g., Kettle et al., 2009; Land et al., 2013) and this functionality is part of published data processing toolkits (e.g., Shutler et al., 2016; Holding et al., 2019).

The most widely used approach to adjust fCO_2 data to different temperatures (t), used in all the examples above, is based on measurements by Takahashi et al. (1993), who measured the variation of fCO_2 with temperature in one seawater sample from the North Atlantic Ocean (strictly speaking, they measured pCO_2, but the results apply equally to fCO_2). Their measurements indicated that the temperature sensitivity of fCO_2 (denoted υ; Eq. 1) was essentially independent of fCO_2 and temperature (i.e., temperature and $\ln(fCO_2)$ have a linear relationship). This was consistent with earlier measurements by Kanwisher (1960) on a single seawater sample collected from the vicinity of Woods Hole (Massachusetts, USA). Takahashi et al. (1993) also claimed that the value of υ was no different for higher salinity waters, citing unpublished preliminary data.

However, it has long been known that υ is not constant across the ocean. For example, Gordon and Jones (1973) computed υ using a finite difference approach across a range of different temperature, salinity, alkalinity and pH values and found that the variability in υ could be approximately parameterised as a function of pCO_2. Using a similar approach, but with different parameterisations of the equilibrium constants in their marine carbonate system calculations, Weiss et al. (1982) and Copin-Montegut (1988) each fitted υ to functions of fCO_2 and temperature. It has been noted that υ may vary with the dissolved inorganic carbon (T_C) content of seawater (e.g., Takahashi et al., 2002), or more generally the ratio between T_C and total alkalinity (A_T) (e.g., Goyet et al., 1993; Wanninkhof et al., 2022).

There are also several lines of evidence that the relationship between temperature and $\ln(fCO_2)$ is not linear (i.e., υ is not constant for a single, isochemical sample). Takahashi et al. (1993) acknowledged this possibility by fitting $\ln(fCO_2)$ to a quadratic function of temperature as well as their linear function, although they did not give any reason to choose one over the other. The fits of Weiss et al. (1982), Copin-Montegut (1988) and Goyet et al. (1993) included various degrees of polynomial temperature dependence. Calculating how fCO_2 changes with temperature using software tools like CO2SYS (Lewis and Wallace, 1998) also shows a non-linear relationship, but its exact form and how much it deviates from linearity both vary widely depending on which parameterisation for the equilibrium constants of carbonic acid is used (McGillis and Wanninkhof, 2006). Data compiled from multiple cruises where fCO_2 was measured at two different temperatures in an equivalent pair of samples, often with accompanying A_T and T_C, showed that a linear (constant υ) adjustment was insufficiently accurate for Δt greater in magnitude than about 1 °C (Wanninkhof et al., 2022). Wanninkhof et al. (2022) recommended calculating from A_T and T_C in order to make accurate adjustments with greater Δt, using the carbonic acid dissociation constants of Lueker et al. (2000) and borate:chlorinity of Uppström (1974). However, the requirement for a second marine carbonate system parameter other than fCO_2 is a major disadvantage because, thanks to ships of opportunity and the variety of (semi-)autonomous sensors

https://doi.org/10.5194/egusphere-2024-626
Preprint. Discussion started: 5 March 2024

available, seawater fCO_2 is by far the most widely measured marine carbonate system parameter in the ocean and it is often the only one available at a particular observation point.

Given the evidence that the equations of Takahashi et al. (1993) are not sufficiently accurate for the full range of temperature adjustments of fCO_2 required by ocean scientists, why do they remain so widely used? First, they are straightforward to calculate, relying only on variables that will be available with any fCO_2 measurement (i.e., fCO_2 itself and temperature). The more complex existing parameterisations that also fulfil this criterion (e.g., Gordon and Jones, 1973; Weiss et al., 1982; Copin-Montegut, 1988) are not based on up-to-date parameterisations of the carbonic acid dissociation constants, which makes a big difference to the results (McGillis and Wanninkhof, 2006). But a more fundamental impediment is not knowing what form the relationship between temperature and $\ln(fCO_2)$ should be expected to take from a theoretical perspective. Should it be (roughly) linear, thus deviations from linearity indicate problems with the calculations used to solve the marine carbonate system? Or should it be non-linear, thus indicating some deficiency with the measurements of Takahashi et al. (1993) – but then which of the non-linear relationships obtained from the different parameterisations of the carbonic acid dissociation constants should be followed?

Here, we aim to provide this missing theoretical basis by developing a new functional form for how fCO_2 and thus υ vary with temperature, derived from the equations governing the marine carbonate system and the van 't Hoff equation. We compare this new form with υ calculated from a fully resolved marine carbonate system – to which end we have added the calculation of υ to PyCO2SYS (Humphreys et al., 2022) – and with laboratory and field data. We compute uncertainties in υ and temperature-adjusted fCO_2 values due to experimental uncertainties and variability in υ through space and time. We assess the contributions of the different equilibrium constants of the marine carbonate system to υ, especially those for carbonic acid dissociation, and consider the implications for how these constants are parameterised and how these previously separate aspects can be better integrated in future studies for a more accurate and internally consistent understanding of the marine carbonate system.

2 Methods

2.1 Adjusting fCO_2 to a different temperature

2.1.1 General theory

The temperature sensitivity of seawater fCO_2 (υ in units of temperature^{-1}) is the first derivative of the natural logarithm of fCO_2 with respect to temperature (t in °C) under constant total alkalinity (A_T) and dissolved inorganic carbon (T_C) (see Humphreys et al. (2022) and references therein for more detailed definitions of A_T, T_C and fCO_2):

$$\upsilon = \frac{\partial \ln(fCO_2)}{\partial t}\bigg|_{A_T,T_C} \quad (1)$$

noting that here and throughout, fCO_2 must be divided by unit fCO_2 (e.g., 1 µatm if fCO_2 is in µatm) before taking the logarithm. We report υ in units of % °C^{-1} (i.e., 10^{-2} °C^{-1}).

https://doi.org/10.5194/egusphere-2024-626
Preprint. Discussion started: 5 March 2024

To adjust an fCO_2 value from one temperature (t_0) to another (t_1), υ must be integrated across the relevant temperature range:

$$\ln[fCO_2(t_1)] = \ln[fCO_2(t_0)] + Y \quad (2)$$

where Y denotes the integral

$$Y = \int_{t_0}^{t_1} \upsilon \, dt \quad (3)$$

Equivalent to Eq. (2):

$$fCO_2(t_1) = fCO_2(t_0) \times \exp(Y) \quad (4)$$

In order to adjust the temperature of a fCO_2 value using Eq. (4), a function for υ that can be integrated with respect to temperature is therefore needed.

2.1.2 The Takahashi et al. (1993) experiment

Takahashi et al. (1993) attempted to determine υ by measuring how pCO_2 varies with temperature (from 2.1 to 24.5 °C) in one seawater sample with constant A_T (reported as "2270 to 2295" µmol kg^{-1}) and T_C (2074 µmol kg^{-1}). The practical salinity was 35.380. Phosphate and silicate concentrations were reported as zero while noting the possibility of silicate contamination from the sample bottles. The sample had been part of the laboratory intercomparison exercise reported by Poisson et al. (1990).

We determined a more precise A_T for the sample by finding the value that, when paired with the T_C and other parameters above, returned the least-squares best fit to the reported pCO_2 values. When using the Lueker et al. (2000) carbonic acid constants and the borate:chlorinity of Uppström (1974), the A_T thus obtained with PyCO2SYS (Humphreys et al., 2022) was 2263 ± 3 µmol kg^{-1}, although each set of carbonic acid constants returned its own unique A_T. For consistency with modern measurements and the rest of our analysis, we also converted the Takahashi et al. (1993) pCO_2 values into fCO_2, although this makes no meaningful difference to any of our results.

Takahashi et al. (1993) fitted their pCO_2 dataset to linear (subscript l) and quadratic (subscript q) equations (here written in terms of fCO_2):

$$\ln(fCO_2) = b_l t + c_l \quad (5)$$

$$\ln(fCO_2) = a_q t^2 + b_q t + c_q \quad (6)$$

where a, b and c are the fitted coefficients. Differentiating with respect to t yields the following for υ:

$$\upsilon_l = b_l \quad (7)$$

$$\upsilon_q = 2a_q t + b_q \quad (8)$$

Finally, integrating across the relevant temperature range yields Y, following e.g. Takahashi et al. (2009):

$$Y_l = b_l(t_1 - t_0) \quad (9)$$

$$Y_q = a_q(t_1^2 - t_0^2) + b_q(t_1 - t_0) \quad (10)$$

Takahashi et al. (1993) reported values of b_l = 4.23% °C^{-1}, a_q = –0.435% °C^{-2} and b_q = 4.33% °C^{-1} with a root-mean-square deviation (RMSD) of 1.0 µatm in fCO_2 for both fits.

https://doi.org/10.5194/egusphere-2024-626
Preprint. Discussion started: 5 March 2024

2.1.3 Approach using van 't Hoff equation

Takahashi et al. (1993) did not give a theoretical basis for either of the forms (linear and quadratic; Eqs. 5 and 6) that they fitted to their dataset nor did they give any reason to choose one over the other. But, as will be discussed later, the form chosen has an important effect on adjustments, especially over greater Δt (Sect. 3.1), and on uncertainty propagation (Sect. 3.2). Here, we provide the theoretical basis for an alternative form based on equations governing the marine carbonate system and the van 't Hoff equation, which is derived from the well-known thermodynamic equation for the Gibbs free energy of chemical reactions.

Seawater fCO_2 is related to A_T and T_C by (e.g., Humphreys et al., 2018)

$$fCO_2 = \frac{K_2^*}{K_0' K_1^*} \frac{[HCO_3^-]^2}{[CO_3^{2-}]} \quad (11)$$

The asterisks in K_1^* and K_2^* indicate that they are stoichiometric equilibrium constants, based on the substance contents of the equilibrating species, rather than thermodynamic constants based on their activities; the prime symbol in K_0' shows that it is a hybrid equilibrium constant, based on the substance content of CO_2(aq) and the fugacity of CO_2(g) (Zeebe and Wolf-Gladrow, 2001). Following Humphreys et al. (2018), A_T and T_C can be approximated with A_x and T_x, which include only the bicarbonate (HCO_3^-) and carbonate (CO_3^{2-}) terms:

$$A_T \approx A_x = [HCO_3^-] + 2[CO_3^{2-}] \quad (12)$$

$$T_C \approx T_x = [HCO_3^-] + [CO_3^{2-}] \quad (13)$$

In typical seawater, the approximations in Eqs. (12) and (13) are more than 99% accurate for T_C and more than 97% accurate for A_T. These approximations have previously been used to explain how fCO_2 responds to changes in A_T and T_C under constant temperature (Humphreys et al., 2018). Equations (12) and (13) can be rearranged for $[HCO_3^-]$ and $[CO_3^{2-}]$:

$$[HCO_3^-] = 2T_x - A_x \quad (14)$$

$$[CO_3^{2-}] = A_x - T_x \quad (15)$$

Under this approximation, both $[HCO_3^-]$ and $[CO_3^{2-}]$ are thus constant under constant A_x and T_x, so temperature affects fCO_2 only through the $K_2^*/K_0'K_1^*$ term in Eq. (11). To relate this to υ, we need to determine the following:

$$\frac{\mathrm{d}\ln(fCO_2)}{\mathrm{d}t} \approx \frac{\mathrm{d}}{\mathrm{d}t}\ln\left(\frac{K_2^*}{K_0' K_1^*}\right) = \frac{\mathrm{d}\ln K_2^*}{\mathrm{d}t} - \frac{\mathrm{d}\ln K_0'}{\mathrm{d}t} - \frac{\mathrm{d}\ln K_1^*}{\mathrm{d}t} \quad (16)$$

The van 't Hoff equation provides a theoretical basis for the first-order response of equilibrium constants to temperature:

$$\frac{\mathrm{d}\ln K}{\mathrm{d}t} = \frac{\Delta_r H^\ominus}{R t_K^2} \quad (17)$$

where $\Delta_r H^\ominus$ is the standard enthalpy of reaction, R the ideal gas constant and t_K temperature in K. Substituting Eq. (17) into Eq. (16) gives

$$\frac{\mathrm{d}\ln(fCO_2)}{\mathrm{d}t} \approx \upsilon_x = \frac{\Delta_r H_2^\ominus - \Delta_r H_0^\ominus - \Delta_r H_1^\ominus}{R t_K^2} \quad (18)$$

https://doi.org/10.5194/egusphere-2024-626
Preprint. Discussion started: 5 March 2024

$\ln(fCO_2)$ should therefore be proportional to $1/t_K$, rather than to t. Based on reported standard enthalpies of formation at 298.15 K (Ruscic and Bross, 2023), and assuming that these are constant under the temperature range of interest, the numerator in Eq. (18) is 25288 ± 98 J mol^{-1} (Appendix A). Given the approximations involved, Eq. (18) is unlikely to provide correct values for υ in seawater directly by using this value, but it does suggest a revised form that could be fitted to experimental data:

$$\ln(fCO_2) = c_h - \frac{b_h}{Rt_K} \quad (19)$$

Following the same steps taken in Sect. 2.1.2 for the linear and quadratic forms of Takahashi et al. (1993), we find the following:

$$\upsilon_h = \frac{b_h}{Rt_K^2} \quad (20)$$

$$\Upsilon_h = \frac{b_h}{R}\left(\frac{1}{t_{K,0}} - \frac{1}{t_{K,1}}\right) \quad (21)$$

We fitted Eq. (19) to the Takahashi et al. (1993) dataset, optimising residuals in fCO_2 rather than $\ln(fCO_2)$ to avoid implicitly weighting the lower-fCO_2 values more heavily. The least-squares best fit b_h was 28995 ± 235 J mol^{-1}, with an RMSD of 2.9 µatm in fCO_2.

2.2 Uncertainty in the experiment

2.2.1 Propagation equations

To quantify uncertainties in fCO_2 resulting from temperature adjustments one needs to know the uncertainty in υ and Υ for whichever form is being used. Here, we derive uncertainty propagation equations following JCGM (2008) for the linear (Eq. 5), quadratic (Eq. 6) and van 't Hoff (Eq. 19) forms.

For the linear and van 't Hoff forms, uncertainty propagation is straightforward:

$$\sigma^2(\upsilon_l) = \sigma^2(b_l) \quad (22)$$

$$\sigma^2(\Upsilon_l) = \sigma^2(b_l) \times (t_1 - t_0)^2 \quad (23)$$

$$\sigma^2(\upsilon_h) = \frac{\sigma^2(b_h)}{(Rt_K^2)^2} \quad (24)$$

$$\sigma^2(\Upsilon_h) = \frac{\sigma^2(b_h)}{R^2}\left(\frac{1}{t_{K,0}} - \frac{1}{t_{K,1}}\right)^2 \quad (25)$$

where σ^2 is uncertainty expressed as a variance.

For the quadratic form, covariances between the fitted coefficients must be included. In general:

$$\sigma^2(p) = \mathbf{J}(p) \cdot \mathbf{U}_q \cdot \mathbf{J}(p)^T \quad (26)$$

where p is the parameter of interest and the uncertainty matrix for the coefficients is

$$\mathbf{U}_q = \begin{bmatrix} \sigma^2(a_q) & \sigma(a_q, b_q) \\ \sigma(a_q, b_q) & \sigma^2(b_q) \end{bmatrix} \quad (27)$$

https://doi.org/10.5194/egusphere-2024-626
Preprint. Discussion started: 5 March 2024

The Jacobian matrices for υ_q and Y_q are

$$\mathbf{J}(\upsilon_q) = \begin{bmatrix} \frac{\partial \upsilon_q}{\partial a_q} & \frac{\partial \upsilon_q}{\partial b_q} \\ \vdots & \vdots \end{bmatrix} = \begin{bmatrix} 2t & 1 \\ \vdots & \vdots \end{bmatrix} \quad (28)$$

$$\mathbf{J}(Y_q) = \begin{bmatrix} \frac{\partial Y_q}{\partial a_q} & \frac{\partial Y_q}{\partial b_q} \\ \vdots & \vdots \end{bmatrix} = \begin{bmatrix} (t_1^2 - t_0^2) & (t_1 - t_0) \\ \vdots & \vdots \end{bmatrix} \quad (29)$$

Thus for a single measurement, Eq. (26) gives

$$\sigma^2(\upsilon_q) = 4t^2\sigma^2(a_q) + \sigma^2(b_q) + 4t\sigma(a_q, b_q) \quad (30)$$

$$\sigma^2(Y_q) = (t_1^2 - t_0^2)^2\sigma^2(a_q) + (t_1 - t_0)^2\sigma^2(b_q) + 2(t_1^2 - t_0^2)(t_1 - t_0)\sigma(a_q, b_q) \quad (31)$$

Finally, uncertainty in Y can be converted into uncertainty in exp(Y) for use in Eq. (4) with

$$\sigma^2[\exp(Y)] = [\exp(Y)]^2 \times \sigma^2(Y) \quad (32)$$

2.2.2 Uncertainties in fitted parameters

To use the equations in Sect. 2.2.1, the uncertainties in the fitted parameters from Eqs. (5), (6) and (19) must be known. We computed these by running Monte-Carlo simulations of the Takahashi et al. (1993) experiment.

We used the Takahashi et al. (1993) temperature and $f\mathrm{CO_2}$ measurements as the starting point for the simulations. For each iteration of the simulation (total iterations = 10^6), we generated a random number for each of temperature and $f\mathrm{CO_2}$, which were added uniformly across the entire dataset to represent systematic errors (trueness), and then a different random number for each temperature and $f\mathrm{CO_2}$ data point, to represent random errors in each measurement (precision). The distributions used for the random numbers are shown in Table 1. The simulated temperature and $f\mathrm{CO_2}$ values (starting point plus systematic and random errors) were then fitted to Eqs. (5), (6) and (19) separately in each iteration. All the forms of υ and Y were also computed based on the fit at each iteration.

The variances $\sigma^2(b_i)$ and $\sigma^2(b_h)$ and the variance-covariance matrix $\mathbf{U}_q$ (Eq. 27)were computed from the fitted coefficients across the full set of iterations.

2.2.3 Validation of uncertainty propagation

The uncertainty propagation equations in Sect. 2.2.1 have all been validated by two comparisons: first, with the variances of the υ and Y values computed across all the simulations in Sect. 2.2.2, and second, by computing the derivatives required for propagation using automatic differentiation (Maclaurin, 2016) rather than manually. The values from the equations agreed to within 0.01% of those based on the simulations and to within 10^{-12}% with the calculations based on automatic differentiation. The former difference is greater (albeit still negligible) because of non-linearities in the forms of υ that are not accounted for in the first-order derivatives used for uncertainty propagation here. The latter difference is attributable to rounding errors at the limit of computer precision.

Table 1. Uncertainties in temperature and seawater $f\mathrm{CO_2}$ assumed for our Monte-Carlo simulations of the Takahashi et al. (1993) experiment.

https://doi.org/10.5194/egusphere-2024-626
Preprint. Discussion started: 5 March 2024

Parameter	Type	Distribution	Spread*	Source / explanation
Temperature	Random	Uniform	0.01 °C	Temperature reported to two decimal places
	Systematic	Normal	0.005 °C	WOCE-era accuracy for oceanographic temperature measurements
fCO_2	Random	Normal	2 µatm	Paper states this as uncertainty; unclear if referring to accuracy or precision
	Systematic	Normal	2 µatm	As above

*Spread indicates the total range for uniform distributions or the standard deviation for normal distributions, with both distributions centred at zero.

2.3 PyCO2SYS extension and calculations

2.3.1 Calculating υ in PyCO2SYS

In PyCO2SYS, υ can be calculated by finite differences or by automatic differentiation (Maclaurin, 2016). The accuracy of the former depends on the size of the difference used, whereas the latter gives the exact result directly (Humphreys et al., 2022). For consistency with the chemical buffer factors in PyCO2SYS, we used automatic differentiation to calculate υ. We constructed a function that evaluates $\ln(fCO_2)$ from A_T, T_C, t and all other relevant parameters (salinity, pressure, nutrients) and applied automatic differentiation to determine its derivative with respect to temperature. The function runs after A_T and T_C have been determined from whichever pair of known parameters the user provides. This was added to the set of results returned by PyCO2SYS as of v1.8.3 (Humphreys et al., 2024).

Previous versions of PyCO2SYS could already calculate $\partial fCO_2/\partial t$ using forward finite difference derivatives as part of the uncertainty propagation tool. υ can be calculated from $\partial fCO_2/\partial t$:

$$\upsilon = \frac{\partial fCO_2}{\partial t}\,(fCO_2)^{-1} \tag{33}$$

We used the finite-difference $\partial fCO_2/\partial t$ and Eq. (33) to validate the values from automatic differentiation. Across 10^4 random combinations of A_T, T_C, salinity, t, pressure, nutrient contents, and carbonic acid dissociation constant parameterisation, we found that the two approaches were consistent, with a mean absolute difference less than 10^{-4}% °C^{-1} (or 0.01%) and a maximum absolute difference less than 0.1% °C^{-1}. This check has been incorporated into the PyCO2SYS test suite to ensure continued consistency in future versions.

2.3.2 Adjusting fCO_2 to different temperatures

Prior to v1.8.3, PyCO2SYS could already convert fCO_2 (also pCO_2, $[CO_2(aq)]$ or xCO_2) values from one temperature to another when no second carbonate system variable was provided, but only using the quadratic fit of Takahashi et al. (1993). In v1.8.3, we have added the option to use the other methods discussed here instead (i.e., the linear fit of Takahashi et al. (1993) and the van 't Hoff form with several different options for b_h, including its parameterisation in Sect. 2.4).

https://doi.org/10.5194/egusphere-2024-626
Preprint. Discussion started: 5 March 2024

Like in previous versions of PyCO2SYS, the same adjustment is applied if any of pCO_2, $[CO_2(aq)]$ or xCO_2 are given as the single known input parameter, as these can all be inter-converted with each other and with fCO_2 without knowledge of a second marine carbonate system variable (Humphreys et al., 2022).

2.3.3 Components of υ

The effect of temperature on fCO_2 propagates through from all the different equilibrium constants of the marine carbonate system. The total υ is the sum of the partial derivatives with respect to each constant:

$$\upsilon = \sum_K \left(\frac{\partial \ln(fCO_2)}{\partial K} \cdot \frac{\partial K}{\partial t} \right) \quad (34)$$

where K is the set of equilibrium constants and other properties that are sensitive to t and involved in calculating fCO_2 from A_T and T_C, specifically, the CO_2 solubility constant K_0', the carbonic acid dissociation constants K_1^* and K_2^*, the borate equilibrium constant K_B^*, and the water dissociation constant K_w^*. The dissociation constants for phosphoric acid, orthosilicic acid, hydrogen sulfide, ammonia, sulfate and hydrogen fluoride also play a role, but their contributions to υ are negligible, being much less than 1% in the modern surface ocean, so we did not include them further in our analysis. (Their effects are still included in the total υ calculated with automatic differentiation, described in Sect. 2.3.1.)

We used the forward finite difference derivatives calculated by PyCO2SYS (Humphreys et al., 2022) to evaluate $\partial fCO_2/\partial K$ and $\partial K/\partial t$ and combined these with Eq. (33) to quantify the influence of each component on υ.

2.3.4 Additional carbonic acid parameterisation

We incorporated the parameterisation of Papadimitriou et al. (2018) for the carbonic acid dissociation constants into PyCO2SYS. This parameterisation covers a range of temperature (–6 to 25 °C) and salinity (33 to 100) conditions appropriate for sea-ice brines; previously, the lowest valid temperature for any parameterisation in PyCO2SYS was –1.7 °C and the highest salinity was 50. The calculations were tested against the check values provided by Papadimitriou et al. (2018) in their Table 3 and these tests were incorporated into the PyCO2SYS automatic test suite (Humphreys et al., 2022).

2.4 Variability in υ and b_h

We used the OceanSODA-ETZH data product (Gregor and Gruber, 2021; dataset version 5, downloaded 4th December 2023) to investigate spatiotemporal variability in surface ocean υ. We computed υ from the gridded fields of A_T, T_C, t and salinity using PyCO2SYS v1.8.3 (Sect. 2.3). OceanSODA-ETZH does not include nutrient fields, so their concentrations were set to zero, but we do not expect this to affect the results because, as noted in Sect. 2.3, their effects on υ are negligible.

We also used the OceanSODA-ETZH data product to parameterise b_h. At each grid point, we computed the mean across all years separately for each month for temperature, salinity, A_T and T_C. We then used PyCO2SYS to calculate fCO_2 from these variables at 50 evenly spaced temperatures from –1.8 to 35.83 °C (i.e., the range of the OceanSODA-ETZH data

https://doi.org/10.5194/egusphere-2024-626
Preprint. Discussion started: 5 March 2024

product) at each month and grid point. Next, we fit Eq. (19) to the generated t and fCO_2 data to find the best fitting b_h value at each point. Finally, we collated all the b_h values and fitted them using a function of the form

$$b_h = u_0 + u_1 t + u_2 s + u_3 f + u_4 t^2 + u_5 s^2 + u_6 f^2 + u_7 ts + u_8 tf + u_9 sf \quad (35)$$

where s is practical salinity, f is fCO_2 and u_0-u_9 are the fitted coefficients. The coefficients and their variance-covariance matrix are provided in the Supplementary Information (Supp. Tables 1-2). Values of υ computed using Eq. (35) for b_h are denoted υ_p.

Fitting the parameterisation to a data product has an advantage over using regular grids of the predictors in that it guarantees including all combinations of predictors that do occur in the real ocean and avoids combinations that do not. It also causes the fit to be weighted more strongly by more prevalent combinations of conditions, leading to improved performance in global applications. However, some regions are less well represented by this global fit (Supp. Fig. 1), so the user may wish to consider developing a more specialised fit for regionally focused work.

A difficulty with applying our parameterisation of b_h is that in-situ fCO_2 is one of the predictors. This may not always be known (e.g., if discrete measurements were conducted at a fixed temperature in the laboratory), and using a different fCO_2 will not yield an accurate b_h. To mitigate this issue, if in-situ fCO_2 is not known before the conversion, we use the constant b_h fitted to the Takahashi et al. (1993) dataset (Sect. 2.1.3) to preliminarily adjust fCO_2 to the in situ temperature, and then use this preliminary fCO_2 to compute b_h with Eq. (35), before recalculating in situ fCO_2 with the computed b_h. This approach is incorporated into the PyCO2SYS implementation, with the user required to identify whether the input or output condition fCO_2 values represents in-situ conditions for this purpose.

2.5 Open source software

All of the analysis presented here was conducted using the free and open source Python programming language (Python Software Foundation; https://www.python.org/). The main packages used, which are also free and open source, include NumPy (Harris et al., 2020), Autograd (Maclaurin, 2016) and xarray (Hoyer and Hamman, 2017) for data manipulation and general calculations; SciPy (Virtanen et al., 2020) for curve fitting; Matplotlib (Hunter, 2007) and Cartopy (Met Office, 2010) for data visualisation; and PyCO2SYS (Humphreys et al., 2022) for marine carbonate system calculations. Geographical features on maps were drawn using data that are freely available from Natural Earth (https://www.naturalearthdata.com/).

3 Results and discussion

3.1 Functional form of υ

3.1.1 Takahashi et al. (1993) dataset

We begin by considering how well the different approaches to calculating υ agree with each other and with the measurements of Takahashi et al. (1993) (Fig. 1). The linear (υ_l) and quadratic (υ_q) forms agree well with the measurements, so it is not clear which (if either) is more appropriate. There is a meaningful difference between υ_l and υ_q only above about 25 °C (Fig. 1a),

https://doi.org/10.5194/egusphere-2024-626
Preprint. Discussion started: 5 March 2024

where υ_q is lower, meaning that fCO_2 would increase less quickly with warming than suggested by υ_l. For example, adjusting from 25 to 35 °C would give an fCO_2 about 17 µatm lower with υ_q than with υ_l.

The van 't Hoff form calculated using the theoretical b_h based on standard enthalpies of reaction (υ_x) has a rather different pattern that does not fit the measurements well (Fig. 1a). However, fitting b_h to the measurements (υ_h) gives a pattern similar to υ_q but with stronger curvature. Although it agrees with the Takahashi et al. (1993) measurements less well than υ_l and υ_q do, with an RMSD of 2.9 µatm as opposed to ~1 µatm, υ_h still falls within their uncertainty window. Like for υ_q, the most significant deviation from υ_l occurs above 25 °C, where Takahashi et al. (1993) did not report any measurements. Adjusting from 25 to 35 °C would give and fCO_2 about 45 µatm lower with υ_h than with υ_l.

There are 18 different parameterisations of the carbonic acid dissociation constants to choose from in PyCO2SYS and each gives a different pattern for υ. However, they are mostly negatively correlated with temperature, like υ_q and υ_h, so they all give lower fCO_2 at higher temperatures than υ_l does (Supp. Fig. 2). Two of the parameterisations are highlighted here. First, the parameterisation of Millero (1979) (υ_{Mi79}) agrees remarkably well with υ_x (Fig. 1). This parameterisation was designed for zero-salinity freshwater and it excludes many of the non-carbonate equilibria that are active in seawater, such as that of borate. Second, the parameterisations that are (at least partly) based on the measurements of Mehrbach et al. (1973) fit the Takahashi et al. (1993) dataset better than those that do not, with the Lueker et al. (2000) parameterisation (υ_{Lu00}) having one of the best fits (RMSD = 2.6 µatm) and falling within the uncertainty of the measurements (Fig. 1a). The pattern of υ_{Lu00} is virtually identical to υ_h (Fig. 1b), including above 25 °C where there are no data to guide the shape of the υ_h curve.

We suggest two main reasons for the differences between υ_x and υ_h, or equivalently, between υ_{Mi79} and υ_{Lu00}. First, υ_h and υ_{Lu00} include additional equilibria that are not present in υ_x and υ_{Mi79}. Some of these extra equilibria are explicitly part of the alkalinity equation in PyCO2SYS (e.g., borate). Others are implicit, such as the formation of $CaCO_3^0$ and $MgCO_3^0$ ion pairs (Millero and Pierrot, 1998), which are incorporated within $[CO_3^{2-}]$ and K_2^* in PyCO2SYS (Humphreys et al., 2022). Second, the van 't Hoff equation with standard enthalpies of reaction predicts the temperature sensitivity of thermodynamic equilibrium constants. However, chemical equilibria in seawater are modelled using stoichiometric equilibrium constants, which have an additional temperature dependency related to the major ion composition and ionic strength of the solution (Pitzer, 1991). Both reasons would affect υ_h and υ_{Lu00}, hence their deviation from υ_x, but not υ_{Mi79}, which is consistent with υ_x.

https://doi.org/10.5194/egusphere-2024-626
Preprint. Discussion started: 5 March 2024

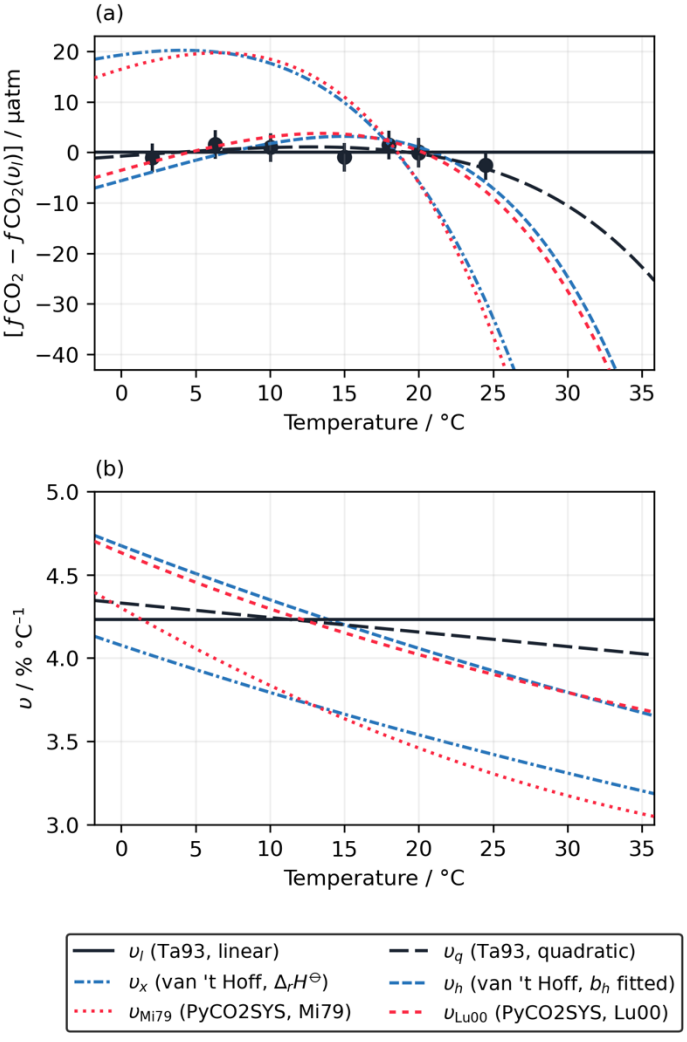

Figure 1: (a) Variation of fCO_2 with temperature according to the measurements of Takahashi et al. (1993) (Ta93; filled circles with vertical 1σ error bars) and the different fitted and theoretical values of υ, all normalised to the linear fit (υ_l) and computed under the conditions of the Takahashi et al. (1993) experiment (Sect. 2.1.2). υ_x is based on Eq. (18), using the theoretical b_h of 25288 J mol^{-1} (Appendix A), while υ_h uses Eq. (19) and the best-fit b_h for the Takahashi et al. (1993) dataset of 28995 J mol^{-1} (Sect. 2.1.3). (b) The values of υ calculated using each of the approaches shown in panel (a) as a function of temperature.

The strong agreement between υ_x and υ_{Mi79} suggests that the approximations made in deriving Eq. (18) are valid (Sect. 2.1.3). The approximations that [CO_2(aq)] is negligible within A_T and T_C (Eqs. 12 and 13) and that the $\Delta_r H^\ominus$ values are constant within the temperature range of interest should hold equally well for υ_h. But the approximation that all non-carbonate species are negligible within A_T (Eq. 12) is more accurate for υ_x and υ_{Mi79} (hence their mutual agreement) than it is for υ_h and υ_{Lu00}. Nevertheless, the strong agreement between υ_h and υ_{Lu00} suggests that the extra equilibria and ionic strength effects can be adequately accounted for by adjusting the value of b_h and without changing the form of the t-ln(fCO_2) relationship.

https://doi.org/10.5194/egusphere-2024-626
Preprint. Discussion started: 5 March 2024

It is unfortunate that the dataset of Takahashi et al. (1993) has a maximum temperature of 24.5 °C, because extra data points above 25 °C could unambiguously distinguish between the different forms of υ. At lower temperatures, the differences between the forms are similar in size to the uncertainty of the measurements, so many more highly accurate measurements would need to be conducted to robustly distinguish between the forms (Fig. 1a). The Kanwisher (1960) measurements covered an even narrower temperature range from 11 to 21.5 °C, which is also insufficient to convincingly show non-linearity.

Nevertheless, we consider that the first-order agreement between the independent υ_x and υ_{Mi79} forms, as well as that between υ_h and υ_{Lu00} – including at higher temperatures where no measurement data exist to guide the υ_h fit – support the new, theoretically justified form for υ in Eq. (19) as being more realistic than the purely empirical linear and quadratic forms proposed by Takahashi et al. (1993), especially for adjustments with greater Δt.

3.1.2 Wanninkhof et al. (2022) compilation

The Wanninkhof et al. (2022) compilation provides much more data (~2000 data points) with which to test the different temperature adjustment approaches, including across variations in salinity and carbonate chemistry (A_T and T_C). The compilation consists of fCO_2 measured in discrete seawater samples at 20 °C (irrespective of the in situ temperature), along with fCO_2 measured at (or close to) the in situ temperature with a continuously flowing underway system at closely corresponding times and locations. Independent measurements of A_T and T_C are also available for many of the data points.

We adjusted the fCO_2 at 20 °C from the discrete samples to the temperature of the in situ measurement using five different approaches: the linear (υ_l) and quadratic (υ_q) equations of Takahashi et al. (1993) (Sect. 2.1.2); the van 't Hoff form with b_h constant as fitted to the Takahashi et al. (1993) dataset (υ_h; Sect. 2.1.3) and parameterised as a function of temperature, salinity and fCO_2 (υ_p; Sect. 2.4); and calculated with PyCO2SYS using T_C as the second known parameter and the carbonic acid dissociation constants of Lueker et al. (2000) (υ_{Lu00}). To compare the accuracy of these adjustments, we computed the rolling mean of the differences between fCO_2 adjusted from 20 °C to the in situ temperature and fCO_2 measured directly at the in situ temperature for each approach, using a ±4 °C window (Fig. 2). Like Wanninkhof et al. (2022), we excluded outliers falling more than ±2 standard deviations from zero, which was 1.4% of the total data points.

For negative Δt there are relatively few data (about 14% of the dataset), such that the different rolling mean lines overlap and mostly fall within the large uncertainty window (Fig. 2). It is not possible to meaningfully distinguish between the different approaches. All appear to overestimate $fCO_2(t_1)$ for Δt from about –14 to –5 °C, by a similar amount to each other, with some falling just outside the uncertainty window of the rolling mean. The consistency between the different approaches here is expected, because they are most similar to each other in the corresponding t_1 range from about 10 to 20 °C (Fig. 1a). The minor deviations for negative Δt are therefore probably due to the sparsity of data in this temperature range, which means that errors due to measurement uncertainty and imperfect co-location of samples are not averaged out. We would expect these deviations from zero to diminish were more data added to the compilation.

The Δt range above 0 °C contains the majority of the dataset (86%) and sufficient data for the approaches to diverge clearly from each other and for some to move well outside the uncertainty window (Fig. 2). Here, the linear form (υ_l)

https://doi.org/10.5194/egusphere-2024-626
Preprint. Discussion started: 5 March 2024

significantly overestimates $fCO_2(t_1)$ as Δt increases. Wanninkhof et al. (2022) tried fitting υ_l directly to this data compilation to improve the accuracy of the adjustment but were not able to resolve this issue. Instead, they concluded that calculations with a fully resolved carbonate system were still required for Δt greater than about 1 °C, recommending the Lueker et al. (2000) carbonic acid dissociation constants with the Uppström (1974) borate:chlorinity for the best agreement (υ_{Lu00}). Like υ_l, the quadratic form (υ_q) overestimates $fCO_2(t_1)$ for positive Δt. The error is about half of that for υ_l, but still well outside the uncertainty window. The van 't Hoff form with constant b_h (υ_h) has a similar error to υ_q, but with the opposite sign (i.e., $fCO_2(t_1)$ is underestimated). However, the van 't Hoff form with a variable, parameterised b_h (υ_p) gives almost perfect agreement even for the largest Δt – performing even better than the calculation with a fully resolved carbonate system (υ_{Lu00}), which also falls just within the uncertainty window.

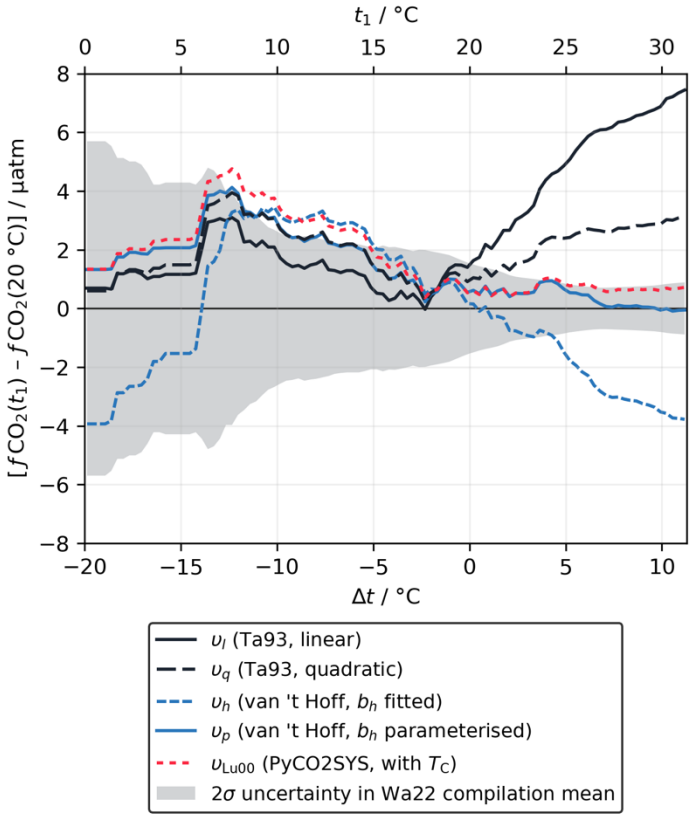

Figure 2: Difference between fCO_2 adjusted from 20 °C to the in situ temperature and a direct measurement at (or close to) the in situ temperature, shown as a rolling mean (window = ±4 °C) for each adjustment approach, for the data in the Wanninkhof et al. (2022) compilation (Wa22). The shaded area shows the 2σ uncertainty in the rolling mean, centred about zero, which is a function of the number of data points within each interval and virtually identical for every approach.

This analysis shows that the van 't Hoff form (υ_h) is at least as capable as the other approaches of adjusting fCO_2 to different temperatures across this data compilation. When variability in b_h is accounted for by the parameterisation proposed in Sect. 2.4,

https://doi.org/10.5194/egusphere-2024-626
Preprint. Discussion started: 5 March 2024

which is completely independent of this data compilation, this approach (υ_p) can be used for accurate Δt adjustments of up to at least 10 °C. However, more data for negative Δt are still essential to improve our confidence in this conclusion across the full temperature range found in the ocean.

Of course, it would be possible to parameterise υ_l and υ_q across the ocean like we have done for υ_h (i.e., υ_p), which would most likely improve their agreement with the data compilation too. However, we have already established that there is no theoretical reason to expect the t-ln(fCO$_2$) relationship to be linear, especially at higher t, and Wanninkhof et al. (2022) tried fitting υ_l to this dataset directly without satisfactory results, so it does not make sense to pursue that approach. Further benefits of υ_h over υ_q are discussed in Sect. 3.2 on uncertainty propagation.

3.1.3 Lueker et al. (2000) parameterisation

When finding the best fitting b_h for a dataset of temperature and ln(fCO$_2$) (Sect. 2.4), with the latter calculated from A_T and T_C using PyCO2SYS and the carbonic acid dissociation constants of Lueker et al. (2000), we find that there are still systematic offsets of up to a few µatm. In other words, Eq. (19) comes close but is not able to exactly reproduce the shape of the ln(fCO$_2$) curve calculated from A_T and T_C with PyCO2SYS (Fig. 3a).

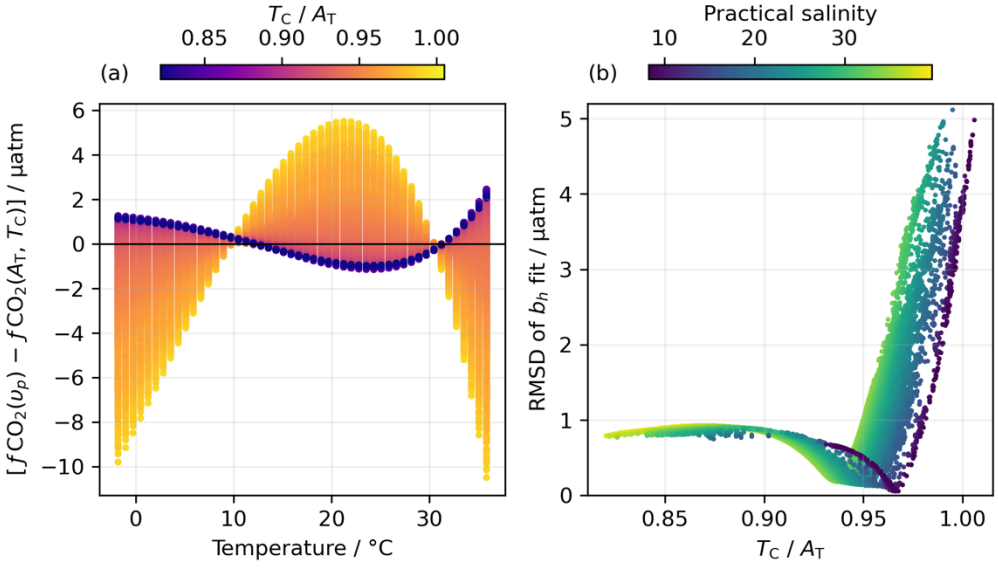

Figure 3: (a) Residuals in fCO$_2$ from finding the best-fitting b_h value at each monthly mean grid point in the OceanSODA-ETZH data product (Sect. 2.4), coloured by T_C/A_T. (b) Variation of the RMSD of the residuals in the b_h fit (in terms of fCO$_2$, as shown in panel a) with T_C/A_T, coloured by practical salinity.

For the majority of the data points (over 97%), the global RMSD for the b_h fit is less than 1 µatm, with the pattern of residuals corresponding to the dark purple points on Fig. 3a. However, the RMSD increases to up to 5 µatm in certain regions and at certain times of year (primarily the Baltic Sea in the winter and the near-coastal Arctic Ocean; Supp. Fig. 1), with an inverted pattern of residuals (Fig. 3a). The RMSD is correlated with several marine carbonate system properties, but one of the strongest

https://doi.org/10.5194/egusphere-2024-626
Preprint. Discussion started: 5 March 2024

correlations is with the ratio between T_C and A_T (Fig. 3b). The RMSD increases to values greater than 1 µatm, correlated with T_C/A_T, for T_C/A_T greater than about 0.95, whereas for lower T_C/A_T, the RMSD is roughly constant at just under 1 µatm. The RMSD drops close to zero between these two regimes, but this is not meaningfully related to some property of chemical buffering in seawater; it is due to the switchover from the residuals being positive at high and low t and negative at intermediate t to the opposite pattern (Fig. 3a).

There are several possible reasons why Eq. (19) cannot exactly reproduce the relationship between t and $\ln(fCO_2)$ calculated using a fully determined carbonate system. The equilibrium constants in PyCO2SYS all include additional temperature-dependent terms beyond the $1/t_K$ term from the van 't Hoff equation (e.g., Weiss, 1974; Dickson, 1990; Lueker et al., 2000), so such additional terms may also be required to capture the pattern of $\ln(fCO_2)$ variation with t. Alternatively, there may be errors in how the parameterisations for the various equilibrium constants in PyCO2SYS represent the influence of temperature – Fig. 3 would show different patterns for other parameterisations. However, while these issues might contribute a component of the discrepancy – i.e., the main pattern with RMSD ~1 µatm seen for T_C/A_T less than ~0.95 – there is no reason to expect their influence to be correlated with T_C/A_T, so they cannot be the entire explanation.

Inaccuracies in the approximations A_x and/or T_x, used in generating Eq. (19), likely also play a role at higher T_C/A_T. The fraction of T_C comprised of $[CO_2(aq)]$, which is ignored in T_x, increases with T_C/A_T, while the fraction of non-carbonate alkalinity, ignored in A_x, decreases with increasing T_C/A_T. Consequently, the approximation that $[HCO_3^-]^2/[CO_3^{2-}]$ is constant across different temperatures (Eq. 16), which emerges from the definitions of A_x and T_x (Eqs. 12-15), becomes less accurate with increasing T_C/A_T. The T_x approximation may be the problem here rather than A_x, because the RMSD of the b_h fit is positively correlated with the error in T_x but negatively correlated with the error in A_x (Supp. Fig. 3).

Although it would be possible to extend Eq. (19) with additional terms to allow a better fit to Lueker et al. (2000), to do so now would be premature. There are major differences between the different carbonic acid parameterisations (e.g., Supp. Fig. 2) that are not yet fully understood. Even though it is the parameterisation given by the best practice guide (Dickson et al., 2007), it is still well-known that Lueker et al. (2000) does not perfectly represent the marine carbonate system to the accuracy with which we can measure it (e.g., Álvarez et al., 2020; Woosley, 2021; Wang et al., 2023; Woosley and Moon, 2023; Carter et al., 2024), and there are outstanding issues to resolve with for example the contribution of organic matter to total alkalinity (e.g., Ulfsbo et al., 2015; Hu, 2020; Kerr et al., 2021) and the borate:chlorinity ratio (e.g., Lee et al., 2010; Fong and Dickson, 2019). Indeed, the parameterised van 't Hoff form agrees slightly better with the Wanninkhof et al. (2022) dataset than does the calculation from T_C and fCO_2 with Lueker et al. (2000) (Fig. 2). Furthermore, there is no robust uncertainty estimate for the equilibrium constants that can be propagated through to determine a meaningful uncertainty in υ_{Lu00} (Orr et al., 2018). The carbonic acid and other equilibrium constant parameterisations are not optimised for this derivative, emergent property (υ) and direct measurements like those of Takahashi et al. (1993), with which more subtle variations about the first-order form in Eq. (19) can be verified, are scarce.

https://doi.org/10.5194/egusphere-2024-626
Preprint. Discussion started: 5 March 2024

3.2 Experimental uncertainty

We performed Monte-Carlo simulations of the Takahashi et al. (1993) experiment (Sect. 2.2.2) to determine the uncertainty in υ computed from that dataset using the linear (υ_l; Eq. 5), quadratic (υ_q; Eq. 6) and van 't Hoff (υ_h; Eq. 19) fits.

Were the linear fit a valid representation of the t-ln(fCO$_2$) relationship, then the 1σ uncertainty in experimentally determined υ_l would be 0.035% °C^{-1}. The biggest contributor (0.028% °C^{-1} on its own) is the precision of the fCO$_2$ measurement, with 0.020% °C^{-1} from systematic bias in fCO$_2$ alone. Systematic biases can affect the slope of the relationship between t and fCO$_2$ because υ is the gradient of the natural logarithm of fCO$_2$ (Eq. 1), which is a non-linear transformation. Temperature uncertainties have a much smaller impact, with 0.001% °C^{-1} uncertainty in υ arising from t precision alone and no effect from t bias. Propagating through to exp(Y_l) for a Δt of +1 °C gives an uncertainty of just under 0.04% (Fig. 4; Supp. Fig. 4). Following Eq. (4), the percentage uncertainty in exp(Y) propagates through to the same percentage uncertainty in the adjusted fCO$_2$ value at t_1, so this calculation is most relevant for understanding how uncertainties in υ affect temperature-adjusted fCO$_2$ values.

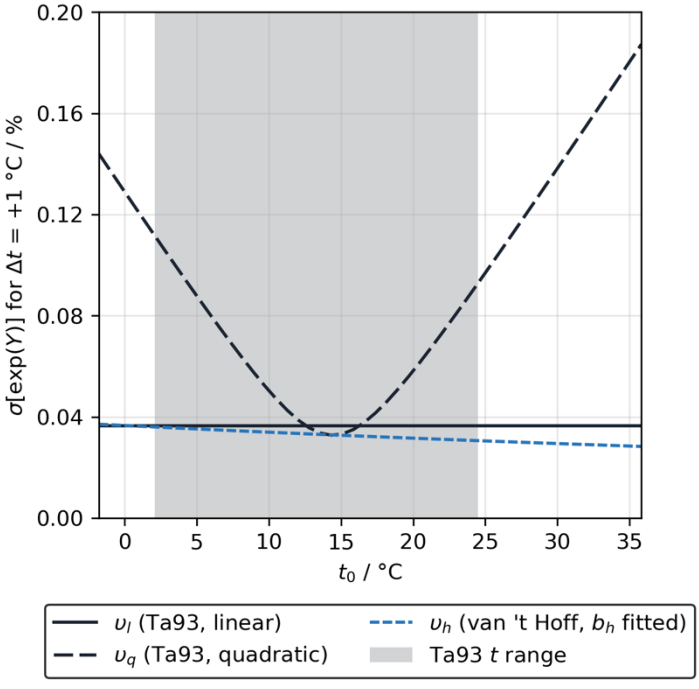

Figure 4: 1σ uncertainty in exp(Y) for Δt = +1 °C, which is equal to the percentage uncertainty in fCO$_2$ at t_1 caused by uncertainty in υ, due to experimental uncertainties in t and fCO$_2$ in the Takahashi et al. (1993) dataset only and fitted with the linear (dotted line; Eq. 5) and quadratic (dashed line; Eq. 6) forms as well as the fitted van 't Hoff form (solid line; Eq. 19). The shaded area shows the range of t from the Takahashi et al. (1993) experiment, while the full t axis range matches OceanSODA-ETZH. The uncertainty in υ itself as a function of temperature has a virtually identical pattern to that shown here for exp(Y) (e.g., an uncertainty in exp(Y) of 0.04%, with Δt = +1 °C, corresponds to an uncertainty in υ of about 0.04% °C^{-1}; Supp. Fig. 4).

https://doi.org/10.5194/egusphere-2024-626
Preprint. Discussion started: 5 March 2024

With the quadratic fit (Eq. 6), the 1σ uncertainty in the slope (b_q) is 0.127% °C^{-1}, in the squared term (a_q) 41.2 × 10^{-6} °C^{-2}, and there is a covariance between these of $\sigma(a_q, b_q)$ = –51 × 10^{-9} °C^{-3}. Propagating through to υ_q and exp(Y_q) gives an uncertainty that is similar to that for the linear fit in the middle of the t range but is up to four times greater in colder and warmer waters (Fig. 4; Supp. Fig. 4). It is essential to include the covariance term for propagation; failure to do so wrongly inflates the final uncertainty.

The van 't Hoff fit has a 1σ uncertainty in b_h of 216.4 J mol^{-1}. Propagating through to υ_h and exp(Y_h) gives a similar uncertainty to that for υ_l, decreasing slightly with increasing temperature (Fig. 4; Supp. Fig. 4).

The uncertainties calculated here, for Δt = +1 °C, are all lower than the "climate quality" target uncertainty for seawater fCO$_2$ measurements of 0.5% proposed by GOA-ON (Newton et al., 2015). This means that this uncertainty component alone would not cause an fCO$_2$(t_1) value with Δt up to ±1 °C to breach this target, regardless of which form was correct, although it is probably not small enough to ignore in a complete uncertainty budget. Also, its contribution scales roughly in proportion with Δt, so for greater Δt this component would become a greater part of the overall uncertainty in fCO$_2$(t_1).

Why do the different approaches have different uncertainties and how do we choose which approach and corresponding uncertainty to use? The linear and van 't Hoff forms both appear to have similarly low uncertainties, but the temperature adjustments that they predict differ from each other by more than the apparent uncertainty windows, especially above 25 °C (Fig. 1). The quadratic form has a completely different uncertainty profile with apparently much greater uncertainty at the edges of the temperature range (Fig. 4). The assumption implicit within any uncertainty calculation that the model being fitted to the data is valid, and that all its adjustable parameters are truly unknown and necessary, is key to resolving this.

As we have shown in Sect. 3.1, it is not consistent with either theory or measurements for υ to be constant and independent from temperature, so the uncertainty calculated for υ_l is valid only under this false premise. In other words, the assumptions that "υ is constant" and "υ varies with temperature" are mutually incompatible. This is how υ_l and υ_h can deviate from each other by more than their apparent uncertainties.

It makes sense that υ_q has greater uncertainty than υ_l and υ_h because υ_q has an extra coefficient to be constrained by the same number of data points. Given more data at higher t, υ_q could plausibly be fitted to a shape almost identical to υ_h, yet still it would appear to have greater uncertainty for this reason. When using υ_q, we accept that there is some curvature in the t-ln(fCO$_2$) relationship, but we implicitly assume that we do not know what form that curvature takes, other than it can be represented by some second-order polynomial. The adjustable parameters that represent the curvature are thus constrained empirically only by the available data, leading to much higher apparent uncertainty towards its edges. But we now know that υ should follow a particular curvature that can be represented with only one adjustable parameter (b_h); it is not an unknown that must be found empirically. The lower uncertainty in υ_h and exp(Y_h) relative to υ_q and exp(Y_q) is therefore more realistic (Fig. 4).

https://doi.org/10.5194/egusphere-2024-626
Preprint. Discussion started: 5 March 2024

While small, this uncertainty component is probably not negligible for the most accurate analyses. More independent reproductions of the Takahashi et al. (1993) experiment, ideally including temperatures up to 35 °C, could reduce this component into a negligible term. However, this component reflects only the experimental uncertainties in fCO_2 and temperature. To use this value as the total uncertainty in υ and/or exp(Y) would be to assume that the single sample measured by Takahashi et al. (1993) is representative of the global ocean. It does not account for spatiotemporal variability in υ, which we discuss in Sect. 3.3.

3.3 Spatial and temporal variability

3.3.1 Variability in υ_{Lu00}

The time-averaged theoretical value of surface ocean υ_{Lu00} in OceanSODA-ETZH (Gregor and Gruber, 2021) follows a latitudinal distribution with lower values near the equator (Fig. 5a). The range in υ_{Lu00} is more than 15% of its mean, from less than 4.0% °C^{-1} to over 4.6% °C^{-1}. The pattern is dominantly driven by temperature. The other variables (A_T, T_C and salinity) together act in the opposite sense, slightly reducing the latitudinal gradient in υ_{Lu00}. This can be seen from the distribution of υ_h, which uses the constant b_h found by fitting to the Takahashi et al. (1993) dataset (Sect. 2.1.3), and which has a similar but stronger latitudinal gradient (Fig. 5b). A counterintuitive consequence of this is that, were the Takahashi et al. (1993) experiment to be repeated systematically across the globe, fitting with a linear equation at each location, then this would return the opposite pattern of υ_l to what we see in Fig. 5a: higher values near the equator and lower near the poles. The variability in υ_l as determined following Takahashi et al. (1993) is independent from the original in situ temperature of the sample, so the experiment would reveal variability in υ only due to the non-thermal parameters.

The seasonal range in υ is a similar size to, although slightly less than, the spatial range in its time-averaged value. It is less than 0.2% °C^{-1} across most of the open ocean, reaching a maximum of just over 0.4% °C^{-1}, or around 10% of the mean, in some near-coastal areas with strong seasonal variability in temperature and/or T_C/A_T (Fig. 5c).

Together, the spatial and seasonal variability in υ_{Lu00} has a standard deviation of 0.23% °C^{-1}. This could be considered to represent the 1σ uncertainty in using a constant υ_l globally, keeping in mind that it has strong regional systematic biases rather than being randomly distributed. It is significantly greater than the apparent experimental uncertainty in υ_l or υ_h of around 0.04% °C^{-1} (Sect. 3.2). Experiments like that of Takahashi et al. (1993) should be sufficiently accurate to detect the variability in υ if conducted at different locations around the global ocean. But it also means that unaccounted-for spatiotemporal variability would lead to several times greater uncertainty in υ and exp(Y) in practice than was computed in Sect. 3.2.

On multi-decadal timescales, υ has been decreasing globally at an average rate of 0.001% °C^{-1} yr^{-1} (Fig. 5d). The decrease has been primarily driven by increasing T_C/A_T with a smaller contribution from warming of the surface ocean. This trend is consistent with that identified by Wanninkhof et al. (2022), and it should lead to a minor decrease in the temperature dependency of surface ocean fCO_2 while atmospheric CO_2 levels continue to rise.

https://doi.org/10.5194/egusphere-2024-626
Preprint. Discussion started: 5 March 2024

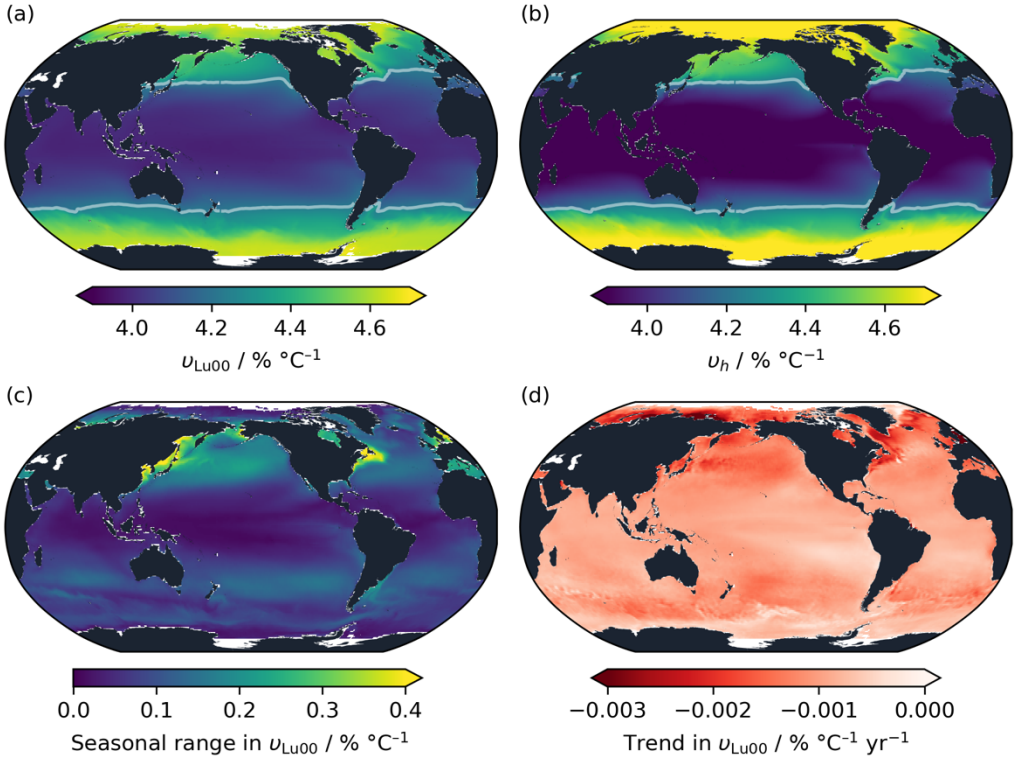

Figure 5: Spatial and temporal variability in υ in OceanSODA-ETZH using the Lueker et al. (2000) parameterisation of the carbonic acid dissociation constants. (a) Theoretical υ_{Lu00} calculated from A_T, T_C and auxiliary variables, averaged through time across the entire OceanSODA-ETZH dataset. (b) υ_h calculated from OceanSODA-ETZH temperature using the b_h value fitted to the Takahashi et al. (1993) measurements, again averaged through time. (a) and (b) are on the same colour scale and the white contour in both shows the Takahashi et al. (1993) linear fit value of υ_l = 4.23% °C^{-1}. (c) Mean seasonal range and (d) multi-decadal trend in υ_{Lu00}.

3.3.2 Components of υ

Variability in υ through space and time arises primarily from the temperature-dependence of the equilibrium constants of the marine carbonate system. Across the contemporary global surface ocean, the biggest contributor to υ is K_0', the solubility constant for CO_2, which typically represents 58–89% of total υ (Fig. 6). The carbonic acid equilibrium constants K_1^* and K_2^* contribute a similar size effect on υ as each other and slightly less than K_0'. However, the K_1^* contribution is always negative and the K_2^* positive, so they partly cancel each other out. Smaller contributions are made by the borate (9–21%) and water (1–8%) equilibria (K_B^* and K_w^*). All other equilibrium constants have a negligible influence on υ in the contemporary ocean, although they might become important at pH values closer to their pK.

Each parameterisation of the carbonic acid dissociation constants gives a different υ distribution but there are some similarities (Fig. 6). We could not identify a link between the functional forms of the parameterisations (i.e., which

https://doi.org/10.5194/egusphere-2024-626
Preprint. Discussion started: 5 March 2024

combinations of t and salinity terms were used) and the distributions shown in Fig. 6; rather, the type of seawater, specific dataset(s) and methodology used to determine the constants were the main controls.

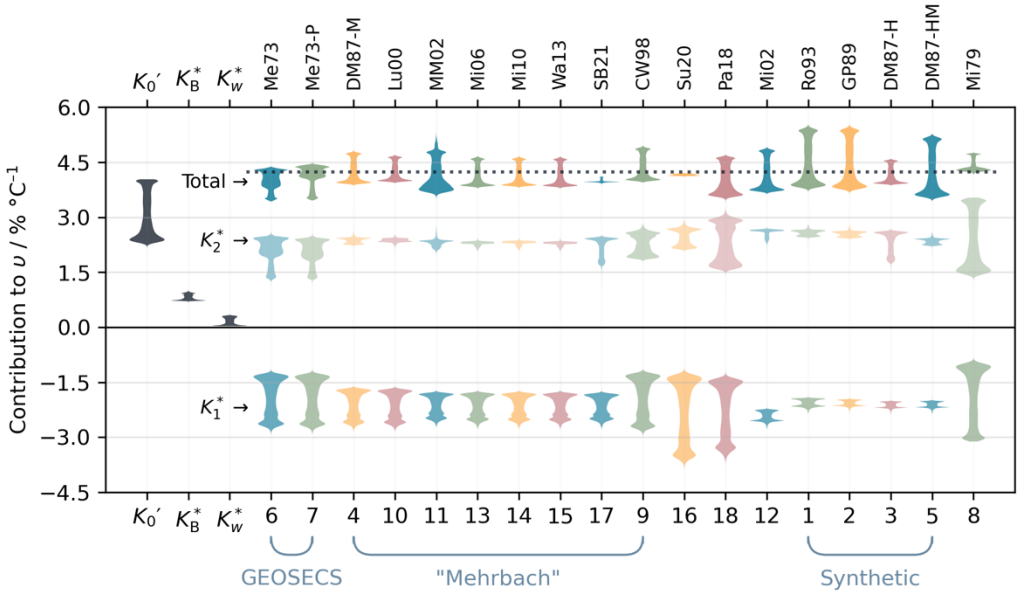

Figure 6: Violin plot of the contributions of each equilibrium system to υ as distributed across the monthly averaged OceanSODA-ETZH data product. From the left, the first three violins show the contributions of the CO_2 solubility constant (K_0') and the borate (K_B^*) and water (K_w^*) equilibria. The remaining columns show the contributions of the carbonic acid dissociation constants K_1^* and K_2^* as well as the total υ for each parameterisation in PyCO2SYS v1.8.3. The horizontal dashed line through the "Total" group is at the Takahashi et al. (1993) linear fit value (υ_l = 4.23% °C^{-1}). The colours are to help the eye track the groups vertically; they do not have any further meaning. The lower horizontal axis shows the option code within PyCO2SYS for the carbonic acid constants, while the upper axis shows an abbreviation of the corresponding study: 1/Ro93 = Roy et al. (1993); 2/GP89 = Goyet and Poisson (1989); 3/DM87-H, 4/DM87-M and 5/DM87-HM = refits of various combinations of Hansson (1973a, b) and Mehrbach et al. (1973) by Dickson and Millero (1987); 6/Me73 and 7/Me73-P = GEOSECS fits of Mehrbach et al. (1973); 8/Mi79 = Millero (1979), for freshwater; 9/CW98 = Cai and Wang (1998); 10/Lu00 = Lueker et al. (2000); 11/MM02 = Mojica Prieto and Millero (2002); 12/Mi02 = Millero et al. (2002); 13/Mi06 = Millero et al. (2006); 14/Mi10 = Millero (2010); 15/Wa13 = Waters and Millero (2013); 16/Su20 = Sulpis et al. (2020); 17/SB21 = Schockman and Byrne (2021); 18/Pa18 = Papadimitriou et al. (2018).

In Fig. 6, the two options labelled "GEOSECS" (6 and 7; Me73 and Me73-P) both use the measurements of Mehrbach et al. (1973), as parameterised by Peng et al. (1987) (because Mehrbach et al. did not provide parameterised functions for their measurements); curiously, total υ with these options has a roughly opposite spatial distribution to all of the other options, with the lowest υ found at high latitudes. Although the GEOSECS options also use different K_B^* and K_w^* parameterisations from all the other options (Humphreys et al., 2022), which modulates the pattern, the inversion is caused by K_1^* and K_2^*. In any case, these options are present in (Py)CO2SYS to reproduce calculations from the GEOSECS era and are not intended for use with modern measurements. Aside from these pair, all other parameterisations based at least in part on the Mehrbach et al. (1973) dataset (labelled "Mehrbach") have similar distributions for K_1^*, K_2^* and total υ. The SB21 parameterisation (Schockman and

https://doi.org/10.5194/egusphere-2024-626
Preprint. Discussion started: 5 March 2024

595 Byrne, 2021) consists of new, spectrophotometric measurements of the product $K_1^*K_2^*$ which were paired with the Waters and Millero (2013) K_1^* to find K_2^*, which resulted in overall virtually zero variability in total υ. This low variability in total υ is echoed by the Su20 parameterisation (Sulpis et al., 2020), which is based on field observations where A_T, T_C, pH and fCO_2 were measured simultaneously, but the low variability is arrived at in a different way, with rather different distributions for the individual K_1^* and K_2^* effects. Parameterisations Pa18 (Papadimitriou et al., 2018), focused on high-salinity, low-temperature
600 sea ice brines, and Mi02 (Millero et al., 2002), based on field measurements, both have similar variability in υ as the "Mehrbach" group.

There is a noticeable difference in the distributions, especially for K_1^*, when moving to the group of parameterisations based on synthetic seawater (Ro93, GP89, DM87-H and DM87-HM; Roy et al., 1993; Goyet and Poisson, 1989; Dickson and Millero, 1987). This suggests that some components of natural seawater that were not replicated in the synthetic seawater used
605 in their experiments may affect the apparent temperature sensitivity of the equilibrium constants being measured, and thus υ. For example, the synthetic seawater recipes used by Goyet and Poisson (1989) and Roy et al. (1993) both did not include any borate, unlike real seawater (Uppström, 1974; Lee et al., 2010). Suspected interactions between borate and carbonate species (Mojica Prieto and Millero, 2002) were not explicitly modelled when evaluating the equilibrium constants, so their effects would be implicitly included within the K_1^* and K_2^* values in real seawater, but not in the synthetic. Dissolved organic matter
610 could also have an equivalent effect. Ultimately, any dissolved species that reacts in an equilibrium with water (i.e., any weak acid or base) or with any component of T_C (i.e., CO_2(aq), HCO_3^- or CO_3^{2-}) could affect υ.

The parameterisation of Mi79 is also shown for completeness, although its distribution is not meaningful because it is intended for zero-salinity freshwater (Millero, 1979).

The parameterisations of K_1^* and K_2^* differ from each other sufficiently that, given the high accuracy with which we
615 can measure fCO_2 and thus experimentally determine υ (Sect. 3.2), more experiments like that of Takahashi et al. (1993) but also including a wider range of temperatures (i.e., at least up to 35 °C) would be a powerful tool to help distinguish between the different parameterisations (Supp. Fig. 2) and diagnose their deficiencies. Such experiments would therefore not only help to better understand υ and its application to adjust fCO_2 data to different temperatures, but could also lead to a more accurate and internally consistent model of the marine carbonate system.

620 **3.3.3 Propagation through to temperature adjustments**

Expressions for υ such as υ_l, υ_q and υ_h are of interest because they can be used to adjust fCO_2 data to different temperatures without knowing a second carbonate system parameter. The variability in υ discussed so far in Sect. 3.3 is therefore most important in terms of how it affects exp(Y) and consequent uncertainty in the adjusted fCO_2 values if ignored.

https://doi.org/10.5194/egusphere-2024-626
Preprint. Discussion started: 5 March 2024

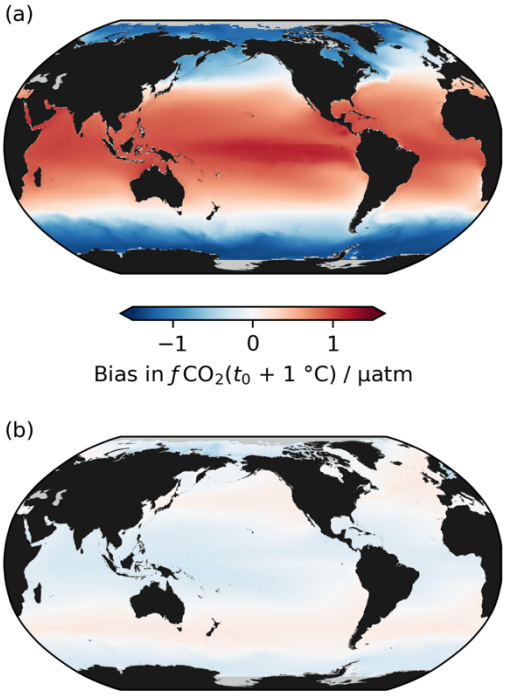

Figure 7: Bias in adjusted fCO_2 for a 1 °C adjustment (Δt = +1 °C) relative to the change in fCO_2 calculated from A_T and T_C with PyCO2SYS and the Lueker et al. (2000) parameterisation of the carbonic acid dissociation constants when the adjustment is applied using (a) the Takahashi et al. (1993) constant υ_l, or (b) the van 't Hoff form with parameterised b_h (Sect. 2.4). The colour scale is the same for (a) and (b).

After a 1 °C warming adjustment from mean surface ocean conditions in OceanSODA-ETZH, both the υ_l and υ_p forms have a global mean bias (relative to the change calculated from A_T and T_C) of less than 0.1 µatm, which is negligible. That the global mean bias is close to zero for υ_l is a coincidence, due to Takahashi et al. (1993) using seawater with roughly average υ_{Lu00} (Fig. 5a). But there are stronger regional biases in υ_l, with 95% of the residuals falling in the range from –1.3 to +1.1 µatm, leading to a global RMSD of 0.8 µatm, or equivalently 0.24% (Fig. 7a). The van 't Hoff form with parameterised b_h (υ_p) has much lower regional biases, with a global RMSD of 0.16 µatm (0.04%) and with 95% of the residuals falling from –0.26 to +0.24 µatm (Fig. 7b). The Takahashi et al. (1993) quadratic fit (υ_q) and the van 't Hoff form with constant b_h fitted to the Takahashi et al. (1993) dataset (υ_h) (both not shown) had negligible global mean biases and intermediate regional biases, with RMSDs of around 0.4 µatm.

The experimental 1σ uncertainty in exp(Y_l) and exp(Y_h) fitted to the Takahashi et al. (1993) dataset was around 0.04% for a 1 °C warming adjustment in both cases (Sect. 3.2). For υ_l, the additional uncertainty from unaccounted-for spatiotemporal variability, plus the fact that the t-ln(fCO_2) relationship is not linear, is therefore four times greater than the experimental uncertainty. For υ_h, the experimental and spatiotemporal uncertainties are about equal in size. Combining these components

https://doi.org/10.5194/egusphere-2024-626
Preprint. Discussion started: 5 March 2024

gives a 1σ uncertainty in adjusted fCO_2 of around 0.06% for υ_p, or 0.24% for υ_l. A 1 °C adjustment with either approach could therefore still meet the GOA-ON climate quality goal of 0.5% (Newton et al., 2015), if other uncertainty components (e.g., in the original fCO_2 measurement at t_0) were small enough. However, the spatiotemporal component of the uncertainty in υ_l results from a known bias with strong regional patterns. Such biases should be eliminated by using a more realistic form of υ (e.g., υ_h rather than υ_l or υ_q, and υ_p or similar to account for variability in υ_h) rather than incorporating them into an overall uncertainty value. But if applying υ_l globally then 0.24% is a reasonable value for the component of uncertainty due to a +1 °C adjustment. It is important to remember that this component is a systematic bias with strong regional patterns when combining it with other components that may be independent for each measurement, because these two types of uncertainty have very different statistical consequences when propagated through to other calculations.

The global biases and the amplitude of spatiotemporal variability scale approximately, but not exactly, with Δt (Fig. 8). The υ_p approach has the lowest RMSD throughout the Δt range, while υ_l has the greatest. υ_q and υ_h have intermediate RMSDs, with that for υ_h significantly lower than υ_q for negative Δt. The RMSDs are generally greater for positive Δt than for negative Δt, which emphasises the need to better understand the temperature sensitivity of fCO_2 and the wider marine carbonate system, particularly at higher temperatures (e.g., Sect. 3.1.1; Woosley, 2021). For a Δt of 10 °C, as might be used in studies unravelling the drivers of seasonal fCO_2 changes, the adjusted fCO_2 would have an uncertainty due to spatiotemporal variability of around 0.8% for υ_p, outside the GOA-ON climate quality goal (0.5%) but well within the weather quality goal of 2.5% (Newton et al., 2015). However, with υ_l, this component of the uncertainty in adjusted fCO_2 would be over 3%, also exceeding the weather quality goal.

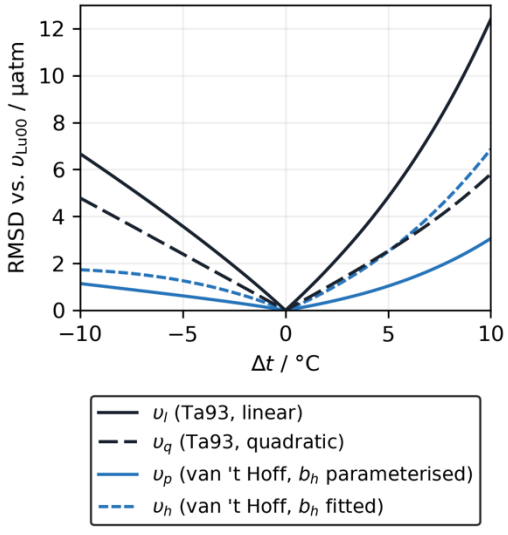

Figure 8: Effect of Δt on the global RMSD of the residuals in the OceanSODA-ETZH data product between fCO_2 adjusted by Δt using the value calculated from A_T and T_C (υ_{Lu00}) and each of υ_l, υ_q, υ_p and υ_h.

https://doi.org/10.5194/egusphere-2024-626
Preprint. Discussion started: 5 March 2024

4 Conclusions

There is no reason to expect a linear relationship between temperature and ln(fCO_2) under isochemical conditions (constant A_T and T_C), as was proposed empirically by Takahashi et al. (1993). Rather, calculations of υ with PyCO2SYS and a theoretical analysis based on the equations governing the marine carbonate system and the van 't Hoff equation each independently suggest that ln(fCO_2) should be proportional to $1/t_K$ to first order. Although this means that the t-ln(fCO_2) relationship does seem to be approximately linear within the temperature range of 2.1 to 24.5 °C measured by Takahashi et al. (1993), it diverges rapidly from linearity at temperatures above 25 °C. The new form of the relationship between temperature and fCO_2 thus proposed here (i.e., υ_h; Eq. 19) is consistent with existing laboratory data (Sect. 3.1.1) and agrees better with field-based datasets than any other approach previously used to adjust seawater fCO_2 to different temperatures (Sect. 3.1.2). υ_h strongly resembles the t-ln(fCO_2) relationship predicted by calculations from A_T and T_C with the carbonic acid dissociation constants of Lueker et al. (2000), although there are still minor discrepancies that could be resolved with more experiments (Sect. 3.1.3).

The uncertainty in υ depends on the method being used to compute it. The Takahashi et al. (1993) experiment gave a 1σ uncertainty of about 0.04% °C^{-1} for the linear form (Sect. 3.2), but this does not account for variability in υ through space and time nor for the fact that the relationship between temperature and ln(fCO_2) is not linear. A 1σ in υ of 0.23% °C^{-1} is therefore more appropriate if using this linear approach (Sect. 3.3.1), which corresponds to 0.24% for fCO_2 adjusted by +1 °C (Sect. 3.3.3). This uncertainty can be reduced by using the new form of t-ln(fCO_2) relationship developed here and parameterising its fitted constant (b_h) as a function of temperature, salinity and fCO_2 (Sect. 2.4), which gives an uncertainty of ±0.06% °C^{-1} for fCO_2 after the same +1 °C adjustment (Sect. 3.3.3). The spatiotemporal components of these uncertainties were computed relative to adjustments calculated from A_T and T_C using PyCO2SYS with the carbonic acid dissociation constants of Lueker et al. (2000) and borate:chlorinity of Uppström (1974), which were the parameterisations that fitted the available datasets the best. While these uncertainties are probably not large enough to have major consequences for global air-sea CO_2 flux budgets, they are not negligible and may be important in regional studies. They should be incorporated into uncertainty budgets and their systematic components should be eliminated by using a more meaningful and accurate form to model the t-ln(fCO_2) relationship, like that proposed here. However, the uncertainty budget is still incomplete: we cannot propagate uncertainties from the equilibrium constants of the marine carbonate system through to υ, because those uncertainties are not yet adequately defined (Orr et al., 2018). It is essential to know the uncertainties and covariances for fitted parameters, not just an uncertainty in the end result, for accurate propagation (Sect. 3.2).

Our parameterisation υ_p is based on a specific set of carbonate system parameterisations. We know that these are not perfect (e.g., Woosley and Moon, 2023; Carter et al., 2024), so our parameterisation of b_h is an intermediate solution. It does agree very well with the available field data (Wanninkhof et al., 2022) upon which it can be tested (and from which it is independent) – indeed, better than any other currently available approach (Sect. 3.1.2) – but we anticipate that it will need to be updated when new data and/or more accurate parameterisations of the marine carbonate system become available. For some

https://doi.org/10.5194/egusphere-2024-626
Preprint. Discussion started: 5 March 2024

applications, accuracy may be improved by developing parameterisations of b_h that are optimised for any particular region(s) of interest.

More measurements like those conducted by Takahashi et al. (1993) to directly determine how fCO_2 varies with temperature under isochemical conditions (i.e., constant A_T and T_C), especially at temperatures above 25 °C where the deviation from υ_l is expected to be greatest, are needed to empirically confirm whether the υ_h form, and indeed calculations from A_T and T_C, are sufficiently accurate. More measurements would show whether discrepancies between υ_p and υ_{Lu00} are due to needing a more sophisticated equation for υ_h with extra fitted parameters, or whether they represent inaccuracies in the Lueker et al. (2000) and other carbonate system parameterisations. Were υ_h to be adapted to include additional fitted parameters, the functional forms included should have a theoretical basis (e.g., Clarke and Glew, 1966) rather than being purely empirical, to ensure accurate uncertainty propagation (Sect. 3.2). Coupling new experiments with pH measurements on the same samples may also help to understand discrepancies raised by (e.g.) Woosley (2021) and Woosley and Moon (2023), such as that different parameterisations of the carbonic acid constants and a different borate:chlorinity work better when comparing A_T and T_C to pH than when comparing them to fCO_2.

We can measure the effect of temperature on fCO_2 accurately enough to distinguish between the different parameterisations of the equilibrium constants and other options (e.g., borate:chlorinity; Humphreys et al., 2022) used when solving the marine carbonate system. Taking this a step further, experimental data like that of Takahashi et al. (1993), Woosley (2021) and Woosley and Moon (2023) could be incorporated when generating these parameterisations. These data constrain the derivatives of the equilibrium constants with respect to temperature, which the parameterisations are not normally optimised for. Constraining these derivatives in the fit would mean the parameterisation can more accurately calculate derivative properties like υ. Such an approach is common in other fields, such as the Pitzer model for chemical activities in aqueous solutions (Pitzer, 1991). There, different measurable properties of the solution constrain the derivatives of fitted coefficients with respect to temperature, pressure and composition, so a single set of coefficients can be found that can accurately calculate all these properties (e.g., Archer, 1992).

At present, including derivative properties in parameterisations would be limited by the scarcity of measurements like those of Takahashi et al. (1993). One possible alternative would be to use data like that compiled by Wanninkhof et al. (2022) and datasets where the marine carbonate system has been overdetermined (i.e., more than two parameters measured) in the field to better parameterise the equilibrium constants (e.g., Sulpis et al., 2020). A practical challenge with this would be that fCO_2 measurements are archived in different compilations (e.g., SOCAT; Bakker et al., 2016) than the other carbonate system variables (e.g., GLODAP; Lauvset et al., 2022) and it is not straightforward to match them back together. However, even were this overcome, this approach would be less useful for parameterising equilibrium constants than using dedicated experiments where well-characterised samples are manipulated under a range of different conditions. In the ocean, temperature is correlated with most other properties, so it would be difficult to isolate which of several correlated drivers was responsible for observed variability. Using these field data to generate parameterisations would also mean that they could no longer be used for independent validation. A better approach would be to reserve field data compilations for testing parameterisations that are

https://doi.org/10.5194/egusphere-2024-626
Preprint. Discussion started: 5 March 2024

based on more carefully controlled laboratory experiments. We expect that combining new experimental measurements with field data in this way and interpreting the results through the lens of the new theoretical basis for υ developed in this study will lead to more accurate temperature adjustments of seawater fCO_2 measurements and contribute to a more internally consistent understanding of the marine carbonate system.

Appendix A: Standard enthalpies of reaction

The reactions corresponding to the equilibrium constants of interest are (Humphreys et al., 2022)

$$CO_2(g) \overset{K_0'}{\rightleftharpoons} CO_2(aq) \quad \text{(A1)}$$

$$CO_2(aq) + H_2O \overset{K_1^*}{\rightleftharpoons} HCO_3^- + H^+ \quad \text{(A2)}$$

$$HCO_3^- \overset{K_2^*}{\rightleftharpoons} CO_3^{2-} + H^+ \quad \text{(A3)}$$

The standard enthalpies of formation ($\Delta_f H^\ominus$) for the relevant species are given in Table A1.

Table A1: Standard enthalpies of formation at 298.15 K following Ruscic and Bross (2023).

Species	**$\Delta_f H^\ominus$ / J mol^{-1}**
CO_2(g)	–393 476 ± 15
CO_2(aq)	–413 196 ± 19
H_2O(l)	–285 800 ± 22
HCO_3^-(aq)	–689 862 ± 39
CO_3^{2-}(aq)	–675 160 ± 53
H^+(aq)	0 (by definition)

Using Hess's law, the standard enthalpies of reaction for Eqs. (A1)-(A3), as used in Eq. (18), are therefore

$$\Delta_r H_0^\ominus = \Delta_f H^\ominus[CO_2(aq)] - \Delta_f H^\ominus[CO_2(g)] = -19\,720 \text{ J mol}^{-1} \quad \text{(A4)}$$

$$\Delta_r H_1^\ominus = \Delta_f H^\ominus(HCO_3^-) + \Delta_f H^\ominus(H^+) - \Delta_f H^\ominus[CO_2(aq)] - \Delta_f H^\ominus(H_2O) = 9\,134 \text{ J mol}^{-1} \quad \text{(A5)}$$

$$\Delta_r H_2^\ominus = \Delta_f H^\ominus(CO_3^{2-}) + \Delta_f H^\ominus(H^+) - \Delta_f H^\ominus(HCO_3^-) = 14\,702 \text{ J mol}^{-1} \quad \text{(A6)}$$

Summing Eqs. (A4)-(A6) as required by Eq. (18) and propagating the uncertainties listed in Table A1 gives a value of $\Delta_r H_2^\ominus - \Delta_r H_0^\ominus - \Delta_r H_1^\ominus = 25288 \pm 98$ kJ mol^{-1}.

https://doi.org/10.5194/egusphere-2024-626
Preprint. Discussion started: 5 March 2024

Code availability

The code for the updated version of PyCO2SYS (v1.8.3) is freely available on GitHub and archived on Zenodo (Humphreys et al., 2024) and can be installed in Python using either pip or conda (via conda-forge). The code used for the rest of the analysis in this manuscript will be made available via GitHub and Zenodo upon final publication.

Author contribution

MPH conducted all aspects of the study.

Competing interests

The author declares that he has no conflict of interest.

Acknowledgements

This manuscript was inspired by discussions during the "Series of workshops on surface ocean pCO_2 observations, synthesis and data products" held at the Flanders Marine Institute (VLIZ) in November 2023. We are indebted to the authors of the previous studies that collected and made available the data used here, especially the measurements of Takahashi et al. (1993), the compilation of Wanninkhof et al. (2022) and the OceanSODA-ETZH data product (Gregor and Gruber, 2021).

References

Álvarez, M., Fajar, N. M., Carter, B. R., Guallart, E. F., Pérez, F. F., Woosley, R. J., and Murata, A.: Global Ocean Spectrophotometric pH Assessment: Consistent Inconsistencies, Environ. Sci. Technol., 54, 10977–10988, https://doi.org/10.1021/acs.est.9b06932, 2020.

Archer, D. G.: Thermodynamic Properties of the NaCl + H_2O System. II. Thermodynamic Properties of NaCl(aq), NaCl·2H_2(cr), and Phase Equilibria, J. Phys. Chem. Ref. Data, 21, 793–829, https://doi.org/10.1063/1.555915, 1992.

Bakker, D. C. E., Pfeil, B., Landa, C. S., Metzl, N., O'Brien, K. M., Olsen, A., Smith, K., Cosca, C., Harasawa, S., Jones, S. D., Nakaoka, S.-I., Nojiri, Y., Schuster, U., Steinhoff, T., Sweeney, C., Takahashi, T., Tilbrook, B., Wada, C., Wanninkhof, R., Alin, S. R., Balestrini, C. F., Barbero, L., Bates, N. R., Bianchi, A. A., Bonou, F., Boutin, J., Bozec, Y., Burger, E. F., Cai, W.-J., Castle, R. D., Chen, L., Chierici, M., Currie, K., Evans, W., Featherstone, C., Feely, R. A., Fransson, A., Goyet, C., Greenwood, N., Gregor, L., Hankin, S., Hardman-Mountford, N. J., Harlay, J., Hauck, J., Hoppema, M., Humphreys, M. P., Hunt, C. W., Huss, B., Ibánhez, J. S. P., Johannessen, T., Keeling, R., Kitidis, V., Körtzinger, A., Kozyr, A., Krasakopoulou, E., Kuwata, A., Landschützer, P., Lauvset, S. K., Lefèvre, N., Lo Monaco, C., Manke, A., Mathis, J. T., Merlivat, L., Millero, F. J., Monteiro, P. M. S., Munro, D. R., Murata, A., Newberger, T., Omar, A. M., Ono, T., Paterson, K., Pearce, D., Pierrot, D., Robbins, L. L., Saito, S., Salisbury, J., Schlitzer, R., Schneider, B., Schweitzer, R., Sieger, R., Skjelvan, I., Sullivan, K. F., Sutherland, S. C., Sutton, A. J., Tadokoro, K., Telszewski, M., Tuma, M., van Heuven, S. M. A. C., Vandemark, D., Ward, B.,

https://doi.org/10.5194/egusphere-2024-626
Preprint. Discussion started: 5 March 2024

Watson, A. J., and Xu, S.: A multi-decade record of high-quality fCO_2 data in version 3 of the Surface Ocean CO_2 Atlas (SOCAT), Earth Syst. Sci. Data, 8, 383–413, https://doi.org/10.5194/essd-8-383-2016, 2016.

Cai, W.-J. and Wang, Y.: The chemistry, fluxes, and sources of carbon dioxide in the estuarine waters of the Satilla and Altamaha Rivers, Georgia, Limnol. Oceanogr., 43, 657–668, https://doi.org/10.4319/lo.1998.43.4.0657, 1998.

Carter, B. R., Sharp, J. D., Dickson, A. G., Álvarez, M., Fong, M. B., García-Ibáñez, M. I., Woosley, R. J., Takeshita, Y., Barbero, L., Byrne, R. H., Cai, W.-J., Chierici, M., Clegg, S. L., Easley, R. A., Fassbender, A. J., Fleger, K. L., Li, X., Martín-Mayor, M., Schockman, K. M., and Wang, Z. A.: Uncertainty sources for measurable ocean carbonate chemistry variables, Limnol. Oceanogr., 69, 1–21, https://doi.org/10.1002/lno.12477, 2024.

Clarke, E. C. W. and Glew, D. N.: Evaluation of thermodynamic functions from equilibrium constants, Trans. Faraday Soc., 62, 539–547, https://doi.org/10.1039/TF9666200539, 1966.

Copin-Montegut, C.: A new formula for the effect of temperature on the partial pressure of CO_2 in seawater, Mar. Chem., 25, 29–37, https://doi.org/10.1016/0304-4203(88)90012-6, 1988.

Dickson, A. G.: Thermodynamics of the dissociation of boric acid in synthetic seawater from 273.15 to 318.15 K, Deep-Sea Res. Pt A, 37, 755–766, https://doi.org/10.1016/0198-0149(90)90004-F, 1990.

Dickson, A. G. and Millero, F. J.: A comparison of the equilibrium constants for the dissociation of carbonic acid in seawater media, Deep-Sea Res. Pt A, 34, 1733–1743, https://doi.org/10.1016/0198-0149(87)90021-5, 1987.

Dickson, A. G., Sabine, C. L., and Christian, J. R. (Eds.): Guide to Best Practices for Ocean CO_2 Measurements, PICES Special Publication 3, 191 pp., 2007.

Dong, Y., Bakker, D. C. E., Bell, T. G., Huang, B., Landschützer, P., Liss, P. S., and Yang, M.: Update on the Temperature Corrections of Global Air-Sea CO_2 Flux Estimates, Global Biogeochem. Cycles, 36, e2022GB007360, https://doi.org/10.1029/2022GB007360, 2022.

Feely, R. A., Takahashi, T., Wanninkhof, R., McPhaden, M. J., Cosca, C. E., Sutherland, S. C., and Carr, M.-E.: Decadal variability of the air-sea CO_2 fluxes in the equatorial Pacific Ocean, J. Geophys. Res. Oceans, 111, https://doi.org/10.1029/2005JC003129, 2006.

Fong, M. B. and Dickson, A. G.: Insights from GO-SHIP hydrography data into the thermodynamic consistency of CO_2 system measurements in seawater, Mar. Chem., 211, 52–63, https://doi.org/10.1016/j.marchem.2019.03.006, 2019.

Friedlingstein, P., O'Sullivan, M., Jones, M. W., Andrew, R. M., Bakker, D. C. E., Hauck, J., Landschützer, P., Le Quéré, C., Luijkx, I. T., Peters, G. P., Peters, W., Pongratz, J., Schwingshackl, C., Sitch, S., Canadell, J. G., Ciais, P., Jackson, R. B., Alin, S. R., Anthoni, P., Barbero, L., Bates, N. R., Becker, M., Bellouin, N., Decharme, B., Bopp, L., Brasika, I. B. M., Cadule, P., Chamberlain, M. A., Chandra, N., Chau, T.-T.-T., Chevallier, F., Chini, L. P., Cronin, M., Dou, X., Enyo, K., Evans, W., Falk, S., Feely, R. A., Feng, L., Ford, D. J., Gasser, T., Ghattas, J., Gkritzalis, T., Grassi, G., Gregor, L., Gruber, N., Gürses, Ö., Harris, I., Hefner, M., Heinke, J., Houghton, R. A., Hurtt, G. C., Iida, Y., Ilyina, T., Jacobson, A. R., Jain, A., Jarníková, T., Jersild, A., Jiang, F., Jin, Z., Joos, F., Kato, E., Keeling, R. F., Kennedy, D., Klein Goldewijk, K., Knauer, J., Korsbakken, J. I., Körtzinger, A., Lan, X., Lefèvre, N., Li, H., Liu, J., Liu, Z., Ma, L., Marland, G., Mayot, N., McGuire, P. C., McKinley, G. A., Meyer, G., Morgan, E. J., Munro, D. R., Nakaoka, S.-I., Niwa, Y., O'Brien, K. M., Olsen, A., Omar, A. M., Ono, T., Paulsen, M., Pierrot, D., Pocock, K., Poulter, B., Powis, C. M., Rehder, G., Resplandy, L., Robertson, E., Rödenbeck, C., Rosan, T. M., Schwinger, J., Séférian, R., et al.: Global Carbon Budget 2023, Earth Syst. Sci. Data, 15, 5301–5369, https://doi.org/10.5194/essd-15-5301-2023, 2023.

Goddijn-Murphy, L. M., Woolf, D. K., Land, P. E., Shutler, J. D., and Donlon, C.: The OceanFlux Greenhouse Gases methodology for deriving a sea surface climatology of CO_2 fugacity in support of air–sea gas flux studies, Ocean Sci., 11, 519–541, https://doi.org/10.5194/os-11-519-2015, 2015.

Gordon, L. I. and Jones, L. B.: The effect of temperature on carbon dioxide partial pressures in seawater, Marine Chemistry, 1, 317–322, https://doi.org/10.1016/0304-4203(73)90021-2, 1973.

Goyet, C. and Poisson, A.: New determination of carbonic acid dissociation constants in seawater as a function of temperature and salinity, Deep-Sea Res. Pt A, 36, 1635–1654, https://doi.org/10.1016/0198-0149(89)90064-2, 1989.

Goyet, C., Millero, F. J., Poisson, A., and Shafer, D. K.: Temperature dependence of CO_2 fugacity in seawater, Mar. Chem., 44, 205–219, https://doi.org/10.1016/0304-4203(93)90203-Z, 1993.

Gregor, L. and Gruber, N.: OceanSODA-ETHZ: a global gridded data set of the surface ocean carbonate system for seasonal to decadal studies of ocean acidification, Earth Syst. Sci. Data, 13, 777–808, https://doi.org/10.5194/essd-13-777-2021, 2021.

Hansson, I.: A new set of acidity constants for carbonic acid and boric acid in sea water, Deep-Sea Res., 20, 461–478, https://doi.org/10.1016/0011-7471(73)90100-9, 1973a.

Hansson, I.: The Determination of Dissociation Constants of Carbonic Acid in Synthetic Sea Water in the Salinity Range of 20–40 ‰ and Temperature Range of 5–30°C, Acta Chem. Scand., 27, 931–944, https://doi.org/10.3891/acta.chem.scand.27-0931, 1973b.

Harris, C. R., Millman, K. J., van der Walt, S. J., Gommers, R., Virtanen, P., Cournapeau, D., Wieser, E., Taylor, J., Berg, S., Smith, N. J., Kern, R., Picus, M., Hoyer, S., van Kerkwijk, M. H., Brett, M., Haldane, A., del Río, J. F., Wiebe, M., Peterson, P., Gérard-Marchant, P., Sheppard, K., Reddy, T., Weckesser, W., Abbasi, H., Gohlke, C., and Oliphant, T. E.: Array programming with NumPy, Nature, 585, 357–362, https://doi.org/10.1038/s41586-020-2649-2, 2020.

Holding, T., Ashton, I. G., Shutler, J. D., Land, P. E., Nightingale, P. D., Rees, A. P., Brown, I., Piolle, J.-F., Kock, A., Bange, H. W., Woolf, D. K., Goddijn-Murphy, L., Pereira, R., Paul, F., Girard-Ardhuin, F., Chapron, B., Rehder, G., Ardhuin, F., and Donlon, C. J.: The FluxEngine air–sea gas flux toolbox: simplified interface and extensions for in situ analyses and multiple sparingly soluble gases, Ocean Sci., 15, 1707–1728, https://doi.org/10.5194/os-15-1707-2019, 2019.

Hoyer, S. and Hamman, J.: xarray: N-D labeled arrays and datasets in Python, J. Open Res. Softw., 5, https://doi.org/10.5334/jors.148, 2017.

Hu, X.: Effect of Organic Alkalinity on Seawater Buffer Capacity: A Numerical Exploration, Aquat. Geochem., 26, 161–178, https://doi.org/10.1007/s10498-020-09375-x, 2020.

Humphreys, M. P.: Climate sensitivity and the rate of ocean acidification: future impacts, and implications for experimental design, ICES J. Mar. Sci., 74, 934–940, https://doi.org/10.1093/icesjms/fsw189, 2017.

Humphreys, M. P., Daniels, C. J., Wolf-Gladrow, D. A., Tyrrell, T., and Achterberg, E. P.: On the influence of marine biogeochemical processes over CO_2 exchange between the atmosphere and ocean, Mar. Chem., 199, 1–11, https://doi.org/10.1016/j.marchem.2017.12.006, 2018.

Humphreys, M. P., Lewis, E. R., Sharp, J. D., and Pierrot, D.: PyCO2SYS v1.8: marine carbonate system calculations in Python, Geosci. Model Dev., 15, 15–43, https://doi.org/10.5194/gmd-15-15-2022, 2022.

Humphreys, M. P., Schiller, A. J., Sandborn, D., Gregor, L., Pierrot, D., van Heuven, S. M. A. C., Lewis, E. R., and Wallace, D. W. R.: PyCO2SYS: marine carbonate system calculations in Python, version 1.8.3, Zenodo, https://doi.org/10.5281/zenodo.10671397, 2024.

Hunter, J. D.: Matplotlib: A 2D graphics environment, Comput. Sci. Eng., 9, 90–95, https://doi.org/10.1109/MCSE.2007.55, 2007.

JCGM: JCGM 100:2008 Evaluation of measurement data — Guide to the expression of uncertainty in measurement, Bureau International des Poids et Mesures, Sèvres, France., 120 pp., 2008.

Jones, D. C., Ito, T., Takano, Y., and Hsu, W.-C.: Spatial and seasonal variability of the air-sea equilibration timescale of carbon dioxide, Global Biogeochem. Cycles, 28, 1163–1178, https://doi.org/10.1002/2014GB004813, 2014.

Kanwisher, J.: pCO_2 in Sea Water and its Effect on the Movement of CO_2 in Nature, Tellus, 12, 209–215, https://doi.org/10.1111/j.2153-3490.1960.tb01302.x, 1960.

Kerr, D. E., Brown, P. J., Grey, A., and Kelleher, B. P.: The influence of organic alkalinity on the carbonate system in coastal waters, Mar. Chem., 237, 104050, https://doi.org/10.1016/j.marchem.2021.104050, 2021.

Kettle, H., Merchant, C. J., Jeffery, C. D., Filipiak, M. J., and Gentemann, C. L.: The impact of diurnal variability in sea surface temperature on the central Atlantic air-sea CO_2 flux, Atmos. Chem. Phys., 9, 529–541, https://doi.org/10.5194/acp-9-529-2009, 2009.

Land, P. E., Shutler, J. D., Cowling, R. D., Woolf, D. K., Walker, P., Findlay, H. S., Upstill-Goddard, R. C., and Donlon, C. J.: Climate change impacts on sea–air fluxes of CO_2 in three Arctic seas: a sensitivity study using Earth observation, Biogeosciences, 10, 8109–8128, https://doi.org/10.5194/bg-10-8109-2013, 2013.

Lauvset, S. K., Lange, N., Tanhua, T., Bittig, H. C., Olsen, A., Kozyr, A., Alin, S., Álvarez, M., Azetsu-Scott, K., Barbero, L., Becker, S., Brown, P. J., Carter, B. R., da Cunha, L. C., Feely, R. A., Hoppema, M., Humphreys, M. P., Ishii, M., Jeansson, E., Jiang, L.-Q., Jones, S. D., Lo Monaco, C., Murata, A., Müller, J. D., Pérez, F. F., Pfeil, B., Schirnick, C., Steinfeldt, R., Suzuki, T., Tilbrook, B., Ulfsbo, A., Velo, A., Woosley, R. J., and Key, R. M.: GLODAPv2.2022: the latest version of the global interior ocean biogeochemical data product, Earth Syst. Sci. Data, 14, 5543–5572, https://doi.org/10.5194/essd-14-5543-2022, 2022.

Lee, K., Kim, T.-W., Byrne, R. H., Millero, F. J., Feely, R. A., and Liu, Y.-M.: The universal ratio of boron to chlorinity for the North Pacific and North Atlantic oceans, Geochim. Cosmochim. Acta, 74, 1801–1811, https://doi.org/10.1016/j.gca.2009.12.027, 2010.

Lewis, E. and Wallace, D. W. R.: Program Developed for CO_2 System Calculations, ORNL/CDIAC-105, Carbon Dioxide Information Analysis Center, Oak Ridge National Laboratory, U.S. Department of Energy, Oak Ridge, TN, USA, https://doi.org/10.15485/1464255, 1998.

Lueker, T. J., Dickson, A. G., and Keeling, C. D.: Ocean pCO_2 calculated from dissolved inorganic carbon, alkalinity, and equations for K_1 and K_2: validation based on laboratory measurements of CO_2 in gas and seawater at equilibrium, Mar. Chem., 70, 105–119, https://doi.org/10.1016/S0304-4203(00)00022-0, 2000.

Maclaurin, D.: Autograd: Automatic Differentiation for Python, in: Modeling, Inference and Optimization with Composable Differentiable Procedures, PhD thesis, Harvard University, Cambridge, MA, 41–57, 2016.

https://doi.org/10.5194/egusphere-2024-626
Preprint. Discussion started: 5 March 2024

McGillis, W. R. and Wanninkhof, R.: Aqueous CO_2 gradients for air–sea flux estimates, Mar. Chem., 98, 100–108, https://doi.org/10.1016/j.marchem.2005.09.003, 2006.

Mehrbach, C., Culberson, C. H., Hawley, J. E., and Pytkowicz, R. M.: Measurement of the Apparent Dissociation Constants of Carbonic Acid in Seawater at Atmospheric Pressure, Limnol. Oceanogr., 18, 897–907, https://doi.org/10.4319/lo.1973.18.6.0897, 1973.

Met Office: Cartopy: a cartographic python library with a Matplotlib interface, Exeter, Devon, 2010.

Metzl, N., Corbière, A., Reverdin, G., Lenton, A., Takahashi, T., Olsen, A., Johannessen, T., Pierrot, D., Wanninkhof, R., Ólafsdóttir, S. R., Olafsson, J., and Ramonet, M.: Recent acceleration of the sea surface fCO_2 growth rate in the North Atlantic subpolar gyre (1993–2008) revealed by winter observations, Global Biogeochem. Cycles, 24, https://doi.org/10.1029/2009GB003658, 2010.

Millero, F. J.: The thermodynamics of the carbonate system in seawater, Geochim. Cosmochim. Acta, 43, 1651–1661, https://doi.org/10.1016/0016-7037(79)90184-4, 1979.

Millero, F. J.: Carbonate constants for estuarine waters, Mar. Freshwater Res., 61, 139–142, https://doi.org/10.1071/MF09254, 2010.

Millero, F. J. and Pierrot, D.: A Chemical Equilibrium Model for Natural Waters, Aquat. Geochem., 4, 153–199, https://doi.org/10.1023/A:1009656023546, 1998.

Millero, F. J., Pierrot, D., Lee, K., Wanninkhof, R., Feely, R., Sabine, C. L., Key, R. M., and Takahashi, T.: Dissociation constants for carbonic acid determined from field measurements, Deep-Sea Res. Pt I, 49, 1705–1723, https://doi.org/10.1016/S0967-0637(02)00093-6, 2002.

Millero, F. J., Graham, T. B., Huang, F., Bustos-Serrano, H., and Pierrot, D.: Dissociation constants of carbonic acid in seawater as a function of salinity and temperature, Mar. Chem., 100, 80–94, https://doi.org/10.1016/j.marchem.2005.12.001, 2006.

Mojica Prieto, F. J. and Millero, F. J.: The values of $pK_1 + pK_2$ for the dissociation of carbonic acid in seawater, Geochim. Cosmochim. Acta, 66, 2529–2540, https://doi.org/10.1016/S0016-7037(02)00855-4, 2002.

Newton, J. A., Feely, R. A., Jewett, E. B., Williamson, P., and Mathis, J.: Global Ocean Acidification Observing Network: Requirements and Governance Plan (2nd Edition), http://goa-on.org/documents/general/GOA-ON_2nd_edition_final.pdf, 2015.

Orr, J. C., Epitalon, J.-M., Dickson, A. G., and Gattuso, J.-P.: Routine uncertainty propagation for the marine carbon dioxide system, Mar. Chem., 207, 84–107, https://doi.org/10.1016/j.marchem.2018.10.006, 2018.

Papadimitriou, S., Loucaides, S., Rérolle, V. M. C., Kennedy, P., Achterberg, E. P., Dickson, A. G., Mowlem, M., and Kennedy, H.: The stoichiometric dissociation constants of carbonic acid in seawater brines from 298 to 267 K, Geochim. Cosmochim. Acta, 220, 55–70, https://doi.org/10.1016/j.gca.2017.09.037, 2018.

Peng, T.-H., Takahashi, T., Broecker, W. S., and Olafsson, J.: Seasonal variability of carbon dioxide, nutrients and oxygen in the northern North Atlantic surface water: observations and a model, Tellus B, 39, 439–458, https://doi.org/10.3402/tellusb.v39i5.15361, 1987.

Pfeil, B., Olsen, A., Bakker, D. C. E., Hankin, S., Koyuk, H., Kozyr, A., Malczyk, J., Manke, A., Metzl, N., Sabine, C. L., Akl, J., Alin, S. R., Bates, N., Bellerby, R. G. J., Borges, A., Boutin, J., Brown, P. J., Cai, W.-J., Chavez, F. P., Chen, A., Cosca, C., Fassbender, A. J., Feely, R. A., González-Dávila, M., Goyet, C., Hales, B., Hardman-Mountford, N., Heinze, C., Hood, M., Hoppema, M., Hunt, C. W., Hydes, D., Ishii, M., Johannessen, T., Jones, S. D., Key, R. M., Körtzinger, A., Landschützer, P., Lauvset, S. K., Lefèvre, N., Lenton, A., Lourantou, A., Merlivat, L., Midorikawa, T., Mintrop, L., Miyazaki, C., Murata, A., Nakadate, A., Nakano, Y., Nakaoka, S., Nojiri, Y., Omar, A. M., Padin, X. A., Park, G.-H., Paterson, K., Perez, F. F., Pierrot, D., Poisson, A., Ríos, A. F., Santana-Casiano, J. M., Salisbury, J., Sarma, V. V. S. S., Schlitzer, R., Schneider, B., Schuster, U., Sieger, R., Skjelvan, I., Steinhoff, T., Suzuki, T., Takahashi, T., Tedesco, K., Telszewski, M., Thomas, H., Tilbrook, B., Tjiputra, J., Vandemark, D., Veness, T., Wanninkhof, R., Watson, A. J., Weiss, R., Wong, C. S., and Yoshikawa-Inoue, H.: A uniform, quality controlled Surface Ocean CO_2 Atlas (SOCAT), Earth Syst. Sci. Data, 5, 125–143, https://doi.org/10.5194/essd-5-125-2013, 2013.

Pierrot, D., Neill, C., Sullivan, K., Castle, R., Wanninkhof, R., Lüger, H., Johannessen, T., Olsen, A., Feely, R. A., and Cosca, C. E.: Recommendations for autonomous underway pCO_2 measuring systems and data-reduction routines, Deep-Sea Res. Pt II, 56, 512–522, https://doi.org/10.1016/j.dsr2.2008.12.005, 2009.

Pitzer, K. S.: Ion Interaction Approach: Theory and Data Correlation, in: Activity Coefficients in Electrolyte Solutions, 2nd Edition, edited by: Pitzer, K. S., CRC Press, Florida, USA, 75–153, 1991.

Poisson, A., Culkin, F., and Ridout, P.: Intercomparison of CO_2 measurements, Deep-Sea Res. Pt A, 37, 1647–1650, https://doi.org/10.1016/0198-0149(90)90067-6, 1990.

Roy, R. N., Roy, L. N., Vogel, K. M., Porter-Moore, C., Pearson, T., Good, C. E., Millero, F. J., and Campbell, D. M.: The dissociation constants of carbonic acid in seawater at salinities 5 to 45 and temperatures 0 to 45°C, Mar. Chem., 44, 249–267, https://doi.org/10.1016/0304-4203(93)90207-5, 1993.

Ruscic, B. and Bross, D.: Active Thermochemical Tables (ATcT) Thermochemical Values ver. 1.130, https://doi.org/10.17038/CSE/1997229, 2023.

Schockman, K. M. and Byrne, R. H.: Spectrophotometric Determination of the Bicarbonate Dissociation Constant in Seawater, Geochim. Cosmochim. Acta, 300, 231–245, https://doi.org/10.1016/j.gca.2021.02.008, 2021.

Shutler, J. D., Land, P. E., Piolle, J.-F., Woolf, D. K., Goddijn-Murphy, L., Paul, F., Girard-Ardhuin, F., Chapron, B., and Donlon, C. J.: FluxEngine: A Flexible Processing System for Calculating Atmosphere–Ocean Carbon Dioxide Gas Fluxes and Climatologies, J. Atmos. Oceanic Technol., 33, 741–756, https://doi.org/10.1175/JTECH-D-14-00204.1, 2016.

Sulpis, O., Lauvset, S. K., and Hagens, M.: Current estimates of K_1* and K_2* appear inconsistent with measured CO_2 system parameters in cold oceanic regions, Ocean Sci., 16, 847–862, https://doi.org/10.5194/os-16-847-2020, 2020.

Takahashi, T., Olafsson, J., Goddard, J. G., Chipman, D. W., and Sutherland, S. C.: Seasonal variation of CO_2 and nutrients in the high-latitude surface oceans: A comparative study, Global Biogeochem. Cycles, 7, 843–878, https://doi.org/10.1029/93GB02263, 1993.

Takahashi, T., Sutherland, S. C., Sweeney, C., Poisson, A., Metzl, N., Tilbrook, B., Bates, N., Wanninkhof, R., Feely, R. A., Sabine, C., Olafsson, J., and Nojiri, Y.: Global sea–air CO_2 flux based on climatological surface ocean pCO_2, and seasonal biological and temperature effects, Deep-Sea Res. Pt II, 49, 1601–1622, https://doi.org/10.1016/S0967-0645(02)00003-6, 2002.

Takahashi, T., Sutherland, S. C., Feely, R. A., and Cosca, C. E.: Decadal Variation of the Surface Water PCO_2 in the Western and Central Equatorial Pacific, Science, 302, 852–856, https://doi.org/10.1126/science.1088570, 2003.

https://doi.org/10.5194/egusphere-2024-626
Preprint. Discussion started: 5 March 2024

Takahashi, T., Sutherland, S. C., Feely, R. A., and Wanninkhof, R.: Decadal change of the surface water pCO_2 in the North Pacific: A synthesis of 35 years of observations, J. Geophys. Res. Oceans, 111, https://doi.org/10.1029/2005JC003074, 2006.

Takahashi, T., Sutherland, S. C., Wanninkhof, R., Sweeney, C., Feely, R. A., Chipman, D. W., Hales, B., Friederich, G., Chavez, F., Sabine, C., Watson, A., Bakker, D. C. E., Schuster, U., Metzl, N., Yoshikawa-Inoue, H., Ishii, M., Midorikawa, T., Nojiri, Y., Körtzinger, A., Steinhoff, T., Hoppema, M., Olafsson, J., Arnarson, T. S., Tilbrook, B., Johannessen, T., Olsen, A., Bellerby, R., Wong, C. S., Delille, B., Bates, N. R., and de Baar, H. J. W.: Climatological mean and decadal change in surface ocean pCO_2, and net sea–air CO_2 flux over the global oceans, Deep-Sea Res. Pt II, 56, 554–577, https://doi.org/10.1016/j.dsr2.2008.12.009, 2009.

Ulfsbo, A., Kuliński, K., Anderson, L. G., and Turner, D. R.: Modelling organic alkalinity in the Baltic Sea using a Humic-Pitzer approach, Mar. Chem., 168, 18–26, https://doi.org/10.1016/j.marchem.2014.10.013, 2015.

Uppström, L. R.: The boron/chlorinity ratio of deep-sea water from the Pacific Ocean, Deep-Sea Res., 21, 161–162, https://doi.org/10.1016/0011-7471(74)90074-6, 1974.

Virtanen, P., Gommers, R., Oliphant, T. E., Haberland, M., Reddy, T., Cournapeau, D., Burovski, E., Peterson, P., Weckesser, W., Bright, J., van der Walt, S. J., Brett, M., Wilson, J., Millman, K. J., Mayorov, N., Nelson, A. R. J., Jones, E., Kern, R., Larson, E., Carey, C. J., Polat, İ., Feng, Y., Moore, E. W., VanderPlas, J., Laxalde, D., Perktold, J., Cimrman, R., Henriksen, I., Quintero, E. A., Harris, C. R., Archibald, A. M., Ribeiro, A. H., Pedregosa, F., van Mulbregt, P., and SciPy 1.0 Contributors: SciPy 1.0: Fundamental Algorithms for Scientific Computing in Python, Nat. Methods, 17, 261–272, https://doi.org/10.1038/s41592-019-0686-2, 2020.

Wang, P., Meng, Q., Xue, L., Zhao, Y., Qiao, H., Hu, H., Wei, Q., Xin, M., Ran, X., Han, C., Zhou, F., and Liu, C.: Preliminary assessment of carbonic acid dissociation constants: Insights from observations in China's east coastal oceans, Mar. Environ. Res., 106219, https://doi.org/10.1016/j.marenvres.2023.106219, 2023.

Wanninkhof, R.: Relationship between wind speed and gas exchange over the ocean revisited: Gas exchange and wind speed over the ocean, Limnol. Oceanogr. Methods, 12, 351–362, https://doi.org/10.4319/lom.2014.12.351, 2014.

Wanninkhof, R., Pierrot, D., Sullivan, K., Mears, P., and Barbero, L.: Comparison of discrete and underway CO_2 measurements: Inferences on the temperature dependence of the fugacity of CO_2 in seawater, Mar. Chem., 247, 104178, https://doi.org/10.1016/j.marchem.2022.104178, 2022.

Waters, J. F. and Millero, F. J.: The free proton concentration scale for seawater pH, Mar. Chem., 149, 8–22, https://doi.org/10.1016/j.marchem.2012.11.003, 2013.

Watson, A. J., Schuster, U., Shutler, J. D., Holding, T., Ashton, I. G. C., Landschützer, P., Woolf, D. K., and Goddijn-Murphy, L.: Revised estimates of ocean-atmosphere CO_2 flux are consistent with ocean carbon inventory, Nat. Commun., 11, 4422, https://doi.org/10.1038/s41467-020-18203-3, 2020.

Weiss, R. F.: Carbon dioxide in water and seawater: the solubility of a non-ideal gas, Mar. Chem., 2, 203–215, https://doi.org/10.1016/0304-4203(74)90015-2, 1974.

Weiss, R. F., Jahnke, R. A., and Keeling, C. D.: Seasonal effects of temperature and salinity on the partial pressure of CO_2 in seawater, Nature, 300, 511–513, https://doi.org/10.1038/300511a0, 1982.

Woosley, R. J.: Evaluation of the temperature dependence of dissociation constants for the marine carbon system using pH and certified reference materials, Mar. Chem., 229, 103914, https://doi.org/10.1016/j.marchem.2020.103914, 2021.

https://doi.org/10.5194/egusphere-2024-626
Preprint. Discussion started: 5 March 2024

Woosley, R. J. and Moon, J.-Y.: Re-evaluation of carbonic acid dissociation constants across conditions and the implications for ocean acidification, Mar. Chem., 250, 104247, https://doi.org/10.1016/j.marchem.2023.104247, 2023.

Zeebe, R. E. and Wolf-Gladrow, D.: CO_2 in Seawater: Equilibrium, Kinetics, Isotopes, Elsevier B.V., Amsterdam, The Netherlands, 346 pp., 2001.

1000